

Online Appendix - Lyx

Artur Carvalho

May 20, 2020

This file contains the paper's additional plots, tables, derivations and a detailed discussion of the numerical approach used to solve the SVM.

Contents

References	1
A Investors' Discount Rate	1
B Optimal RMP-Contingent Payoffs when $\iota = 0$	3
1 Model Results for Varying λ Values in the $\kappa \times \sigma_h$ Plane	5
2 Model Results for Varying κ Values in the $\lambda \times \sigma_h$ Plane	25
C Interpolating the Pre-Volatility Shock Bond Pricing Formula	45
1 The SVM Bond Price Inner Integral	45
2 Independence from the bond contract parameters	47
3 Numerical Computation of the \mathbf{b} -independent f functions	50
4 Calculating the Vector of Bond Prices in the Finite Difference Methods for the Equity Function	51
D Numerical Approach to Joint Equilibria	52
1 Full Information Module	52
2 Misrepresentation Module	53
3 μ_b -Module	54
4 Sub-Module I	56
5 Sub-Module II	58

References

He, Zhiguo, and Wei Xiong, 2012, Rollover Risk and Credit Risk, *Journal of Finance* 67, 391–430, Publisher: Blackwell Publishing Inc.

Appendix A. Investors' Discount Rate

Test: [He and Xiong \(2012\)](#)

LEMMA 1: Consider the setting in section ?? . Let r represent the constant risk-free rate and let S_t denote the time- t fair-value of a traded security. Suppose investors are subject to a liquidity shock that arrives according to a Poisson distribution with intensity ξ . Upon the arrival of the shock, they must immediately liquidate their positions at a fractional cost k to recover $(1 - k)S_t$. Then, the investors' effective discount rate is $r + \xi \cdot k$.

Proof. Let $\{\delta_t : 0 \leq t < \infty\}$ represent the security's cash-flows. The fair-value is given by

$$S_t = \mathbb{E}^{\mathcal{Q}} \left[\int_t^\infty e^{-r(s-t)} d\delta_s \middle| \mathcal{F}_t \right]$$

where superscript \mathcal{Q} denotes expectation in the risk-neutral measure, and $(\mathcal{F}_t)_{t \geq 0}$ is the associated filtration.

Because (i) investors are homogeneous and (ii) liquidity shocks are independent from the security's cash-flows, we can derive investors' valuation S_t^{Inv} by considering the following alternative case: instead of being forced to liquidate their positions, asset holders simply accept a fractional reduction on all future cash-flows whenever a liquidity shock arrives. Denote by $\{N_t : 0 \leq t < \infty\}$ the counting process for the liquidity shocks. It follows that $(1 - k)^{N_t}$ is a compound Poisson process, and S_t^{Inv} is given by:

$$S_t^{Inv} = (1 - k)^{N_t} \mathbb{E}^{\mathcal{Q}} \left[\int_t^\infty e^{-r(s-t)} (1 - k)^{(N_s - N_t)} \cdot d\delta_s \middle| \mathcal{G}_t \right] \quad (\text{A1})$$

where $(\mathcal{G}_t)_{t \geq 0}$ is the market filtration, defined as the filtration for the security's cash-flows \mathcal{F} , augmented by the information on the occurrence of liquidity shocks $\mathcal{H} \equiv \sigma(\{N_u\}, u \leq t)$, so that $\mathcal{G}_t \equiv \mathcal{F}_t \vee \mathcal{H}_t$.

By independence between liquidity shocks and cash-flows, we can write the term on the RHS of equation A1 above as:

$$(1 - k)^{N_t} \mathbb{E}^{\mathcal{Q}} \left[\int_t^\infty \mathbb{E} \left[(1 - k)^{N_s - N_t} \middle| \mathcal{H}_t \right] e^{-r(s-t)} d\delta_s \middle| \mathcal{F}_t \right] = \mathbb{E}^{\mathcal{Q}} \left[\int_t^\infty \mathbb{E} \left[(1 - k)^{N_s} \middle| \mathcal{H}_t \right] e^{-r(s-t)} d\delta_s \middle| \mathcal{F}_t \right]$$

Now consider the process X_t defined as

$$X_t \equiv N_t \log(1 - k) + \xi k t$$

This process has a continuous part $X^c(t) = -\xi k t$, and a pure jump part $J(t) = N(t) \log(1 - k)$. Let $f(X) \equiv e^x$. By the Ito-Doeblin's formula,

$$\begin{aligned} f(X(t)) &= \cancel{f(X(0))} + \xi k \int_0^t f'(X(u)) du + \sum_{0 \leq u \leq t} [f(X(u)) - f(X(u-))] \\ &= 1 + \xi k \int_0^t f(X(u)) du + \sum_{0 \leq u \leq t} \left[(1 - k)^{N(u)} - (1 - k)^{N(u-)} \right] e^{-\xi k u} \\ &= 1 + \xi k \int_0^t f(X(u)) du + \sum_{0 \leq u \leq t} \left[(1 - k)^{\Delta N(u)} - 1 \right] (1 - k)^{N(u-)} e^{-\xi k u} \\ &= 1 + \xi k \int_0^t f(X(u)) du + \sum_{0 \leq u \leq t} [-k \Delta N(u)] f(X(u-)) \end{aligned}$$

The summation on the RHS can be written as

$$\begin{aligned}
\sum_{0 \leq u \leq t} [f(X(u)) - f(X(u-))] &= \sum_{0 \leq u \leq t} \left[(1-k)^{N(u)} - (1-k)^{N(u-)} \right] e^{-\xi k u} \\
&= \sum_{0 \leq u \leq t} \left[(1-k)^{\Delta N(u)} - 1 \right] (1-k)^{N(u-)} e^{-\xi k u} \\
&= \sum_{0 \leq u \leq t} [-k \Delta N(u)] f(X(u-)) \\
&= -k \int_0^t f(X(u-)) dN(u)
\end{aligned}$$

Hence,

$$\begin{aligned}
f(X(t)) &= 1 + k \int_0^t f(X(u-)) [-\xi du + dN(u)] \\
&= 1 + k \int_0^t f(X(u-)) dM(u)
\end{aligned}$$

where M is the compensated Poisson process $M(u) \equiv N(u) - \xi u$. Left-continuity of $f \cdot X$ then implies that $f \cdot X$ is a martingale.

Finally, we are able to solve the expectation term inside the integral:

$$\begin{aligned}
\mathbb{E} \left[(1-k)^{N_s} \mid \mathcal{H}_t \right] &= \mathbb{E} \left[e^{N_s \log(1-k) + \xi k s} e^{-\xi k s} \mid \mathcal{H}_t \right] \\
&= e^{-\xi k s} \mathbb{E} [f(X_s) \mid \mathcal{H}_t] \\
&= e^{-\xi k s} f(X_t) \\
&= (1-k)^{N_t} e^{-\xi k (s-t)}
\end{aligned}$$

Therefore, equation A1 becomes

$$S_t^{Inv} = (1-k)^{N_t} \mathbb{E}^Q \left[\int_t^\infty e^{-(r+\xi k)(s-t)} \cdot d\delta_s \mid \mathcal{F}_t \right]$$

and we see thus that the investors' effective discount rate is indeed $r + \xi \cdot k$. \square

Appendix B. Optimal RMP-Contingent Payoffs when $\iota = 0$

To study the interplay between liquidity in secondary bond markets and firm riskiness, I focus on variations to the transaction costs, shock intensity and jump size parameters, that is, κ , λ and σ_h , respectively. I set the remaining parameters to their values in Table ??, except for σ_l , which is set to 0.15. The results are shown below.

The first set of graphs (figures ?? to ??) shows SVM results in the $(\sigma_h \times \kappa)$ -plane for multiple shock intensity (λ) values. All else constant, a higher volatility shock size makes it more likely the firm defaults before maturity, decreasing the value of the bonds. Likewise, the more illiquid secondary markets are, the more investors discount future debt cash-flows. In either case, debt rollover becomes more costly, forcing the firm to rely more on equity financing. Leverage falls as the firm reduces debt service payments by revising down its principal and coupon. However, the variation in equity value is not commensurate with the fall in the price of debt, so this shift in the

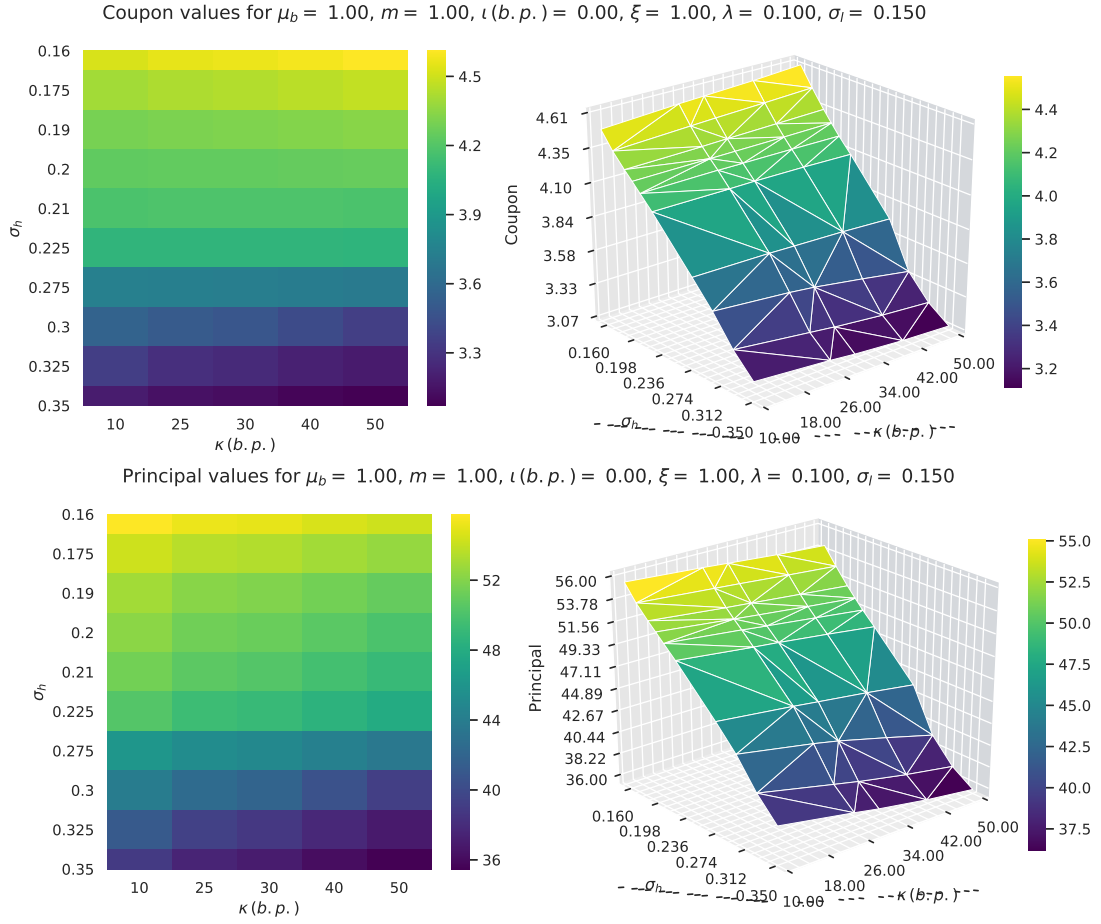
firm's funding mix results in a lower total firm value and a lower return on equity. Additionally, because equity holders become more invested in the firm, the bankruptcy barrier is relaxed.

The optimal capital structure and bankruptcy barrier are much more sensitive to changes in σ_h relative to changes in κ , which is apparent in the color gradients in the heatmaps. Moreover, analogously to the shock size, a higher shock intensity increases the likelihood of default, raising debt rollover costs. Therefore, higher λ makes the effects described above more pronounced. Finally, the interaction between shock intensity and shock size can be seen in the the second set of graphs (figures 6 to 10), where results are displayed in the $(\lambda \times \sigma_h)$ -plane for multiple κ values. An increase in the intensity is akin to a larger shock size: it decreases the firm leverage, the bankruptcy barrier, the total firm value and the return on equity.

B.1 Model Results for Varying λ Values in the $\kappa \times \sigma_h$ Plane

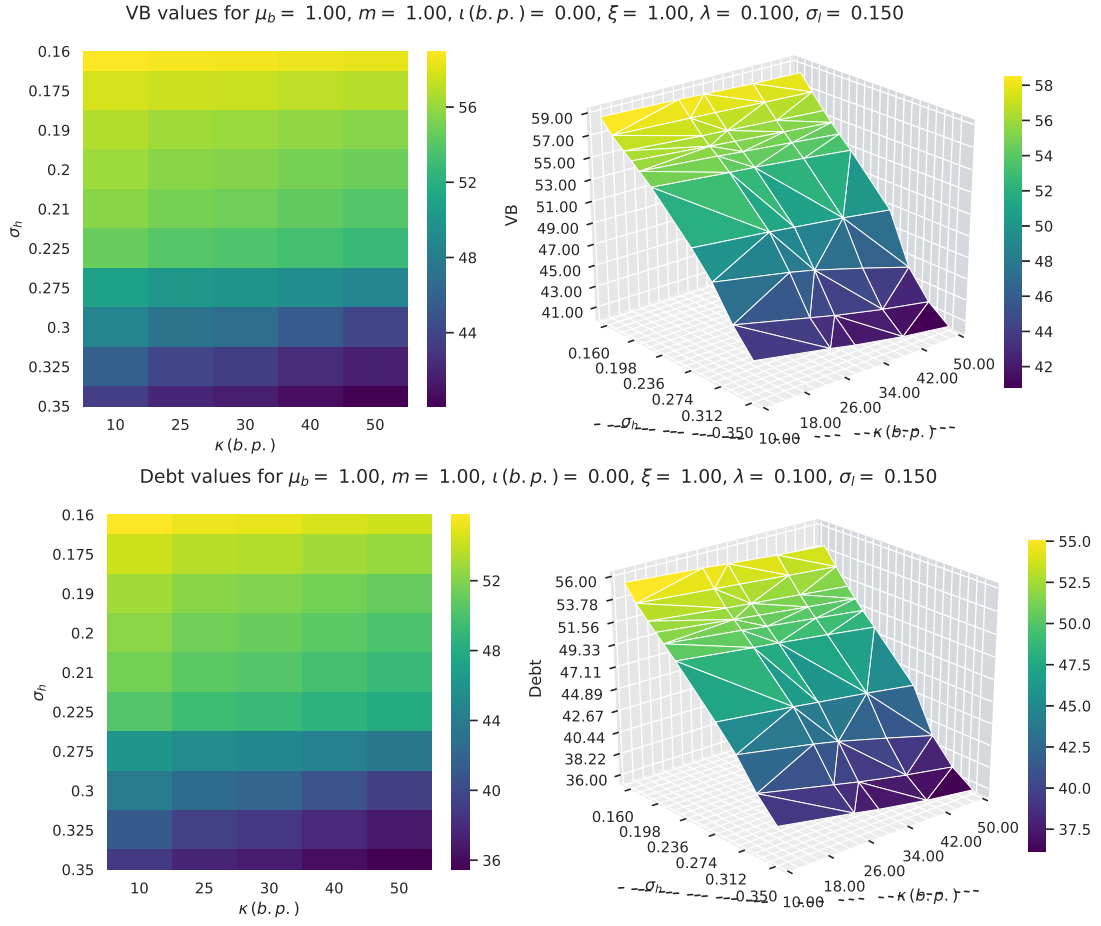
B.1.1 $\lambda = 0.10$

Figure 1. Model Results for $\lambda = 0.100$



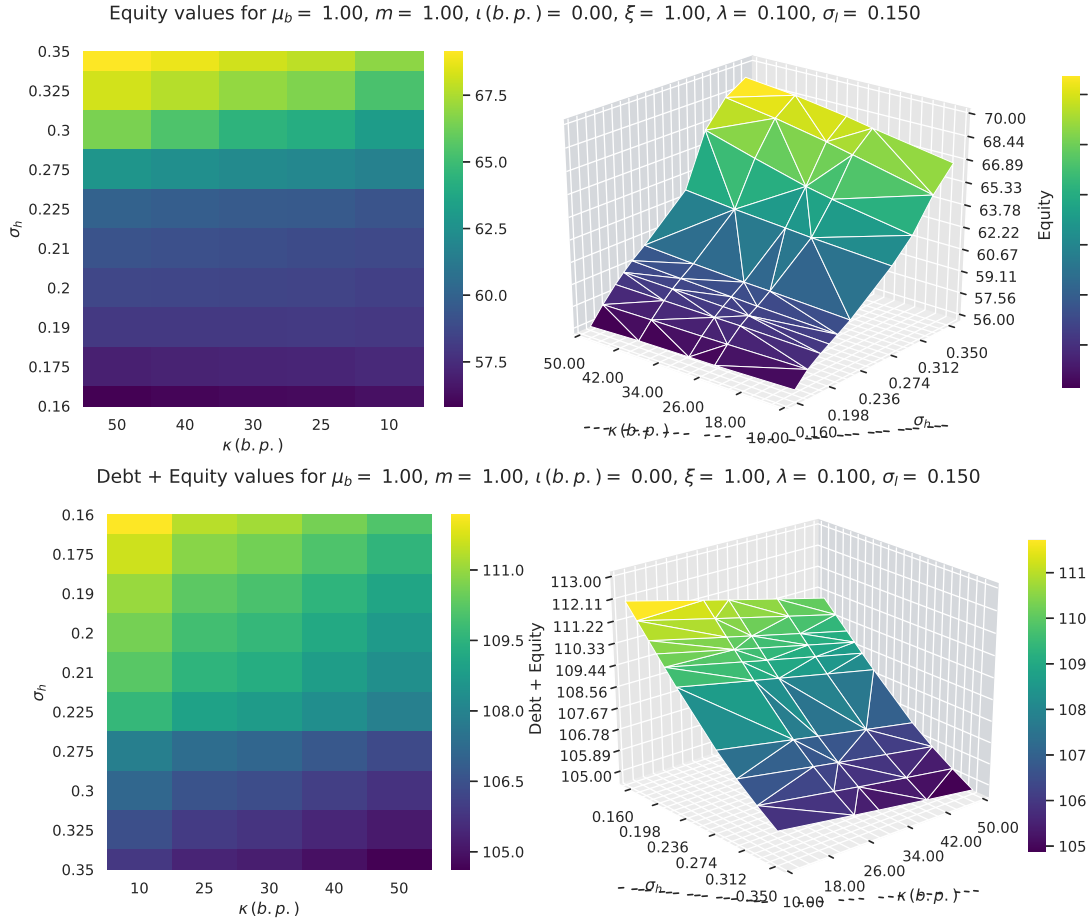
[Continues on the next page.]

Figure 1. Model Results for $\lambda = 0.100$



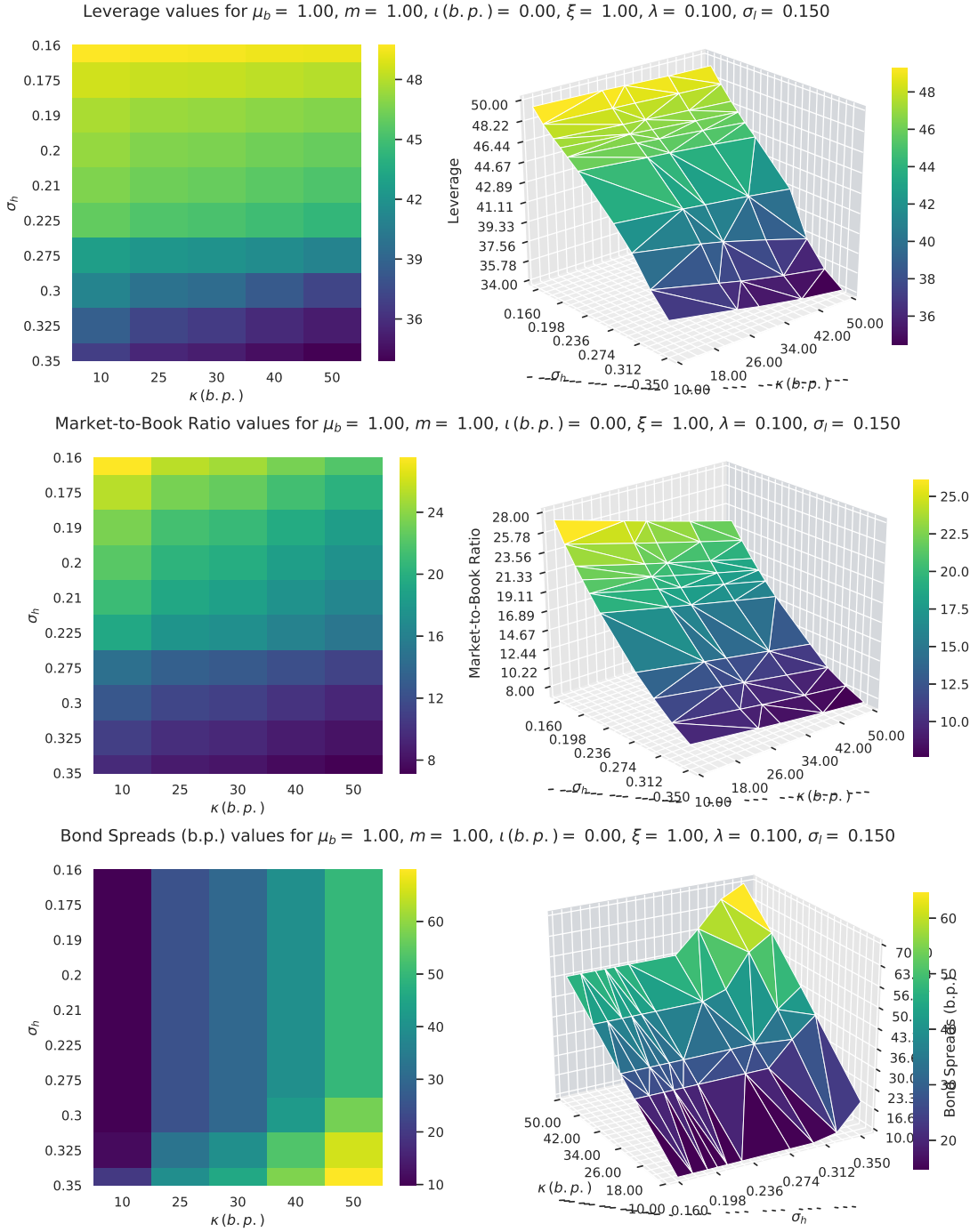
[Continues on the next page.]

Figure 1. Model Results for $\lambda = 0.100$



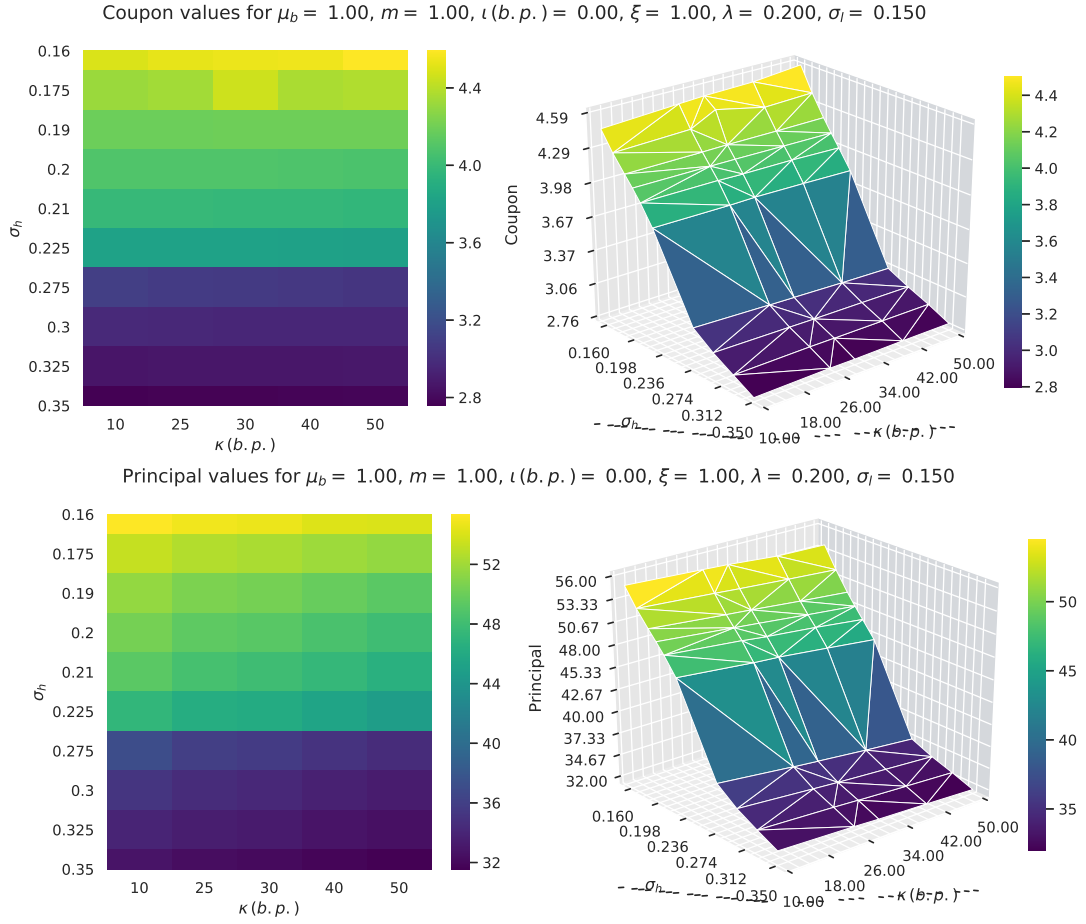
[Continues on the next page.]

Figure 1. Model Results for $\lambda = 0.100$



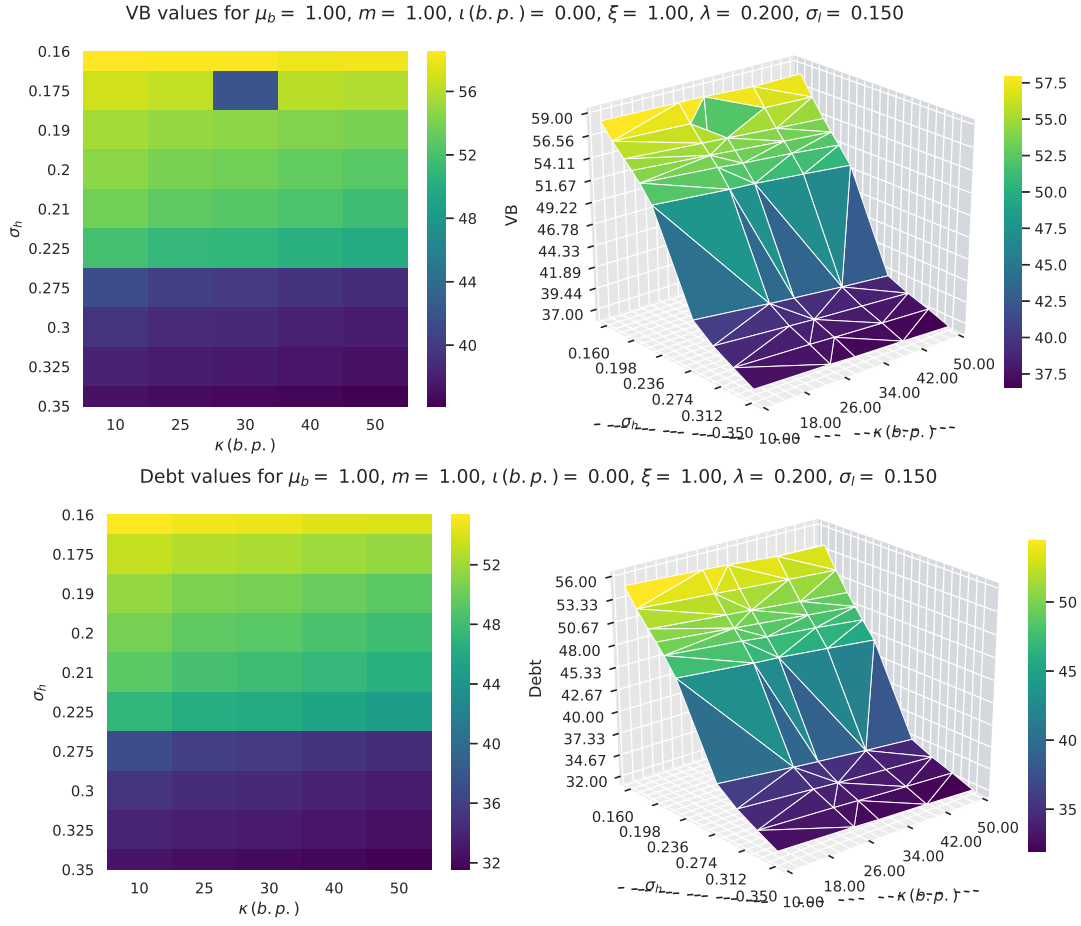
B.1.2 $\lambda = 0.20$

Figure 2. Model Results for $\lambda = 0.200$



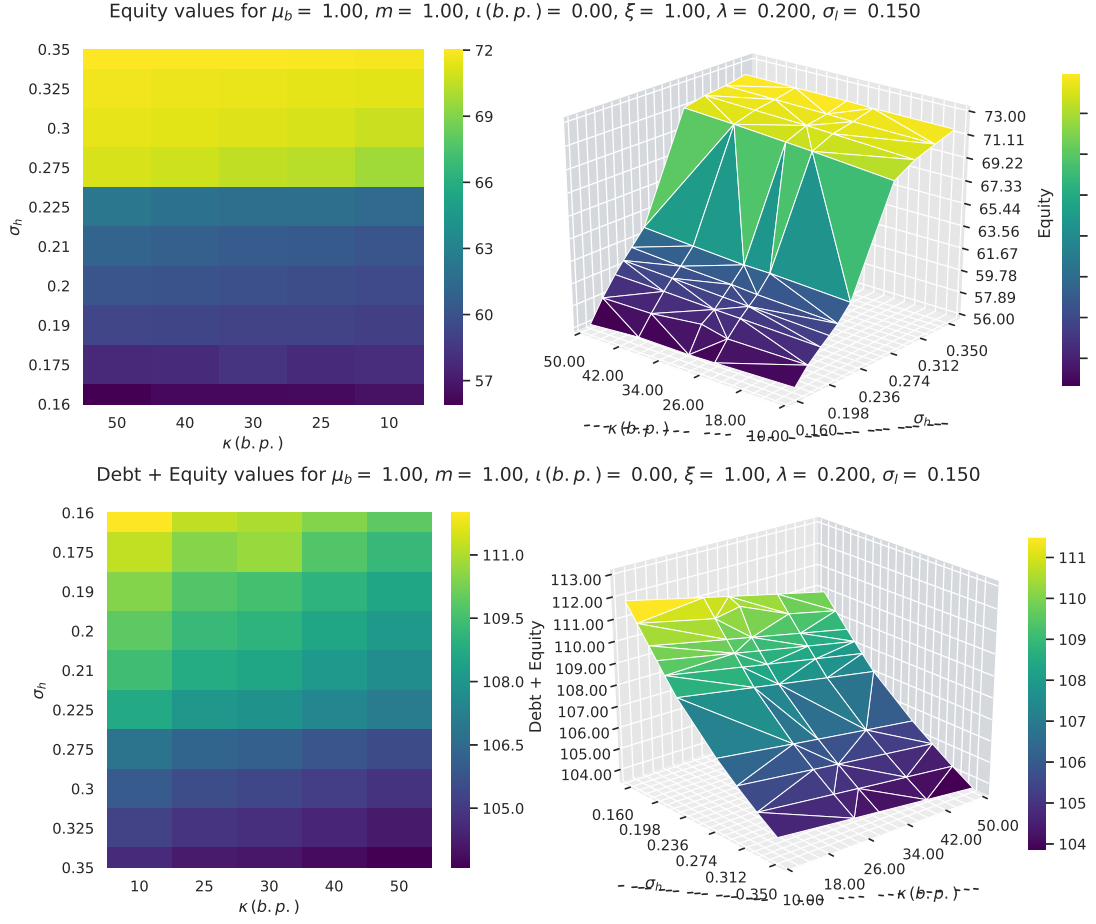
[Continues on the next page.]

Figure 2. Model Results for $\lambda = 0.200$



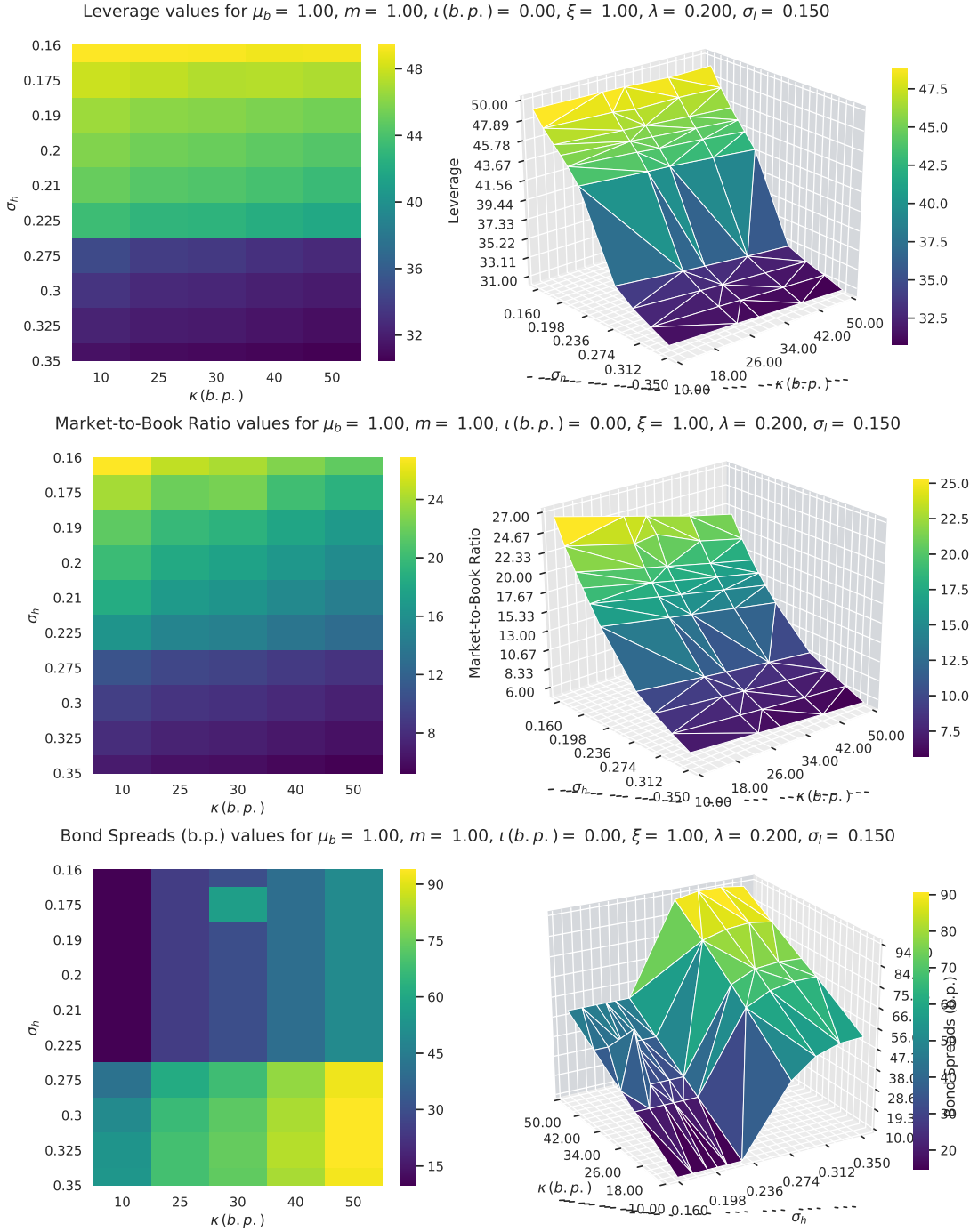
[Continues on the next page.]

Figure 2. Model Results for $\lambda = 0.200$



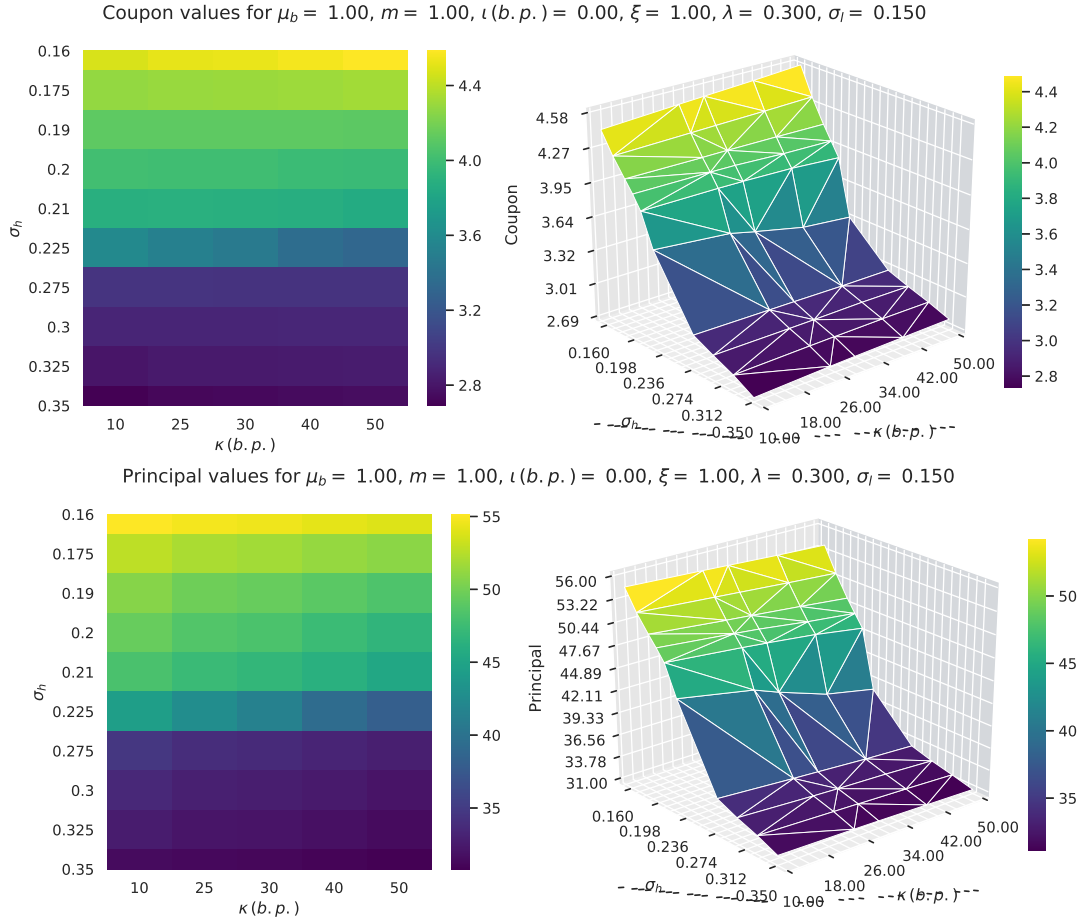
[Continues on the next page.]

Figure 2. Model Results for $\lambda = 0.200$



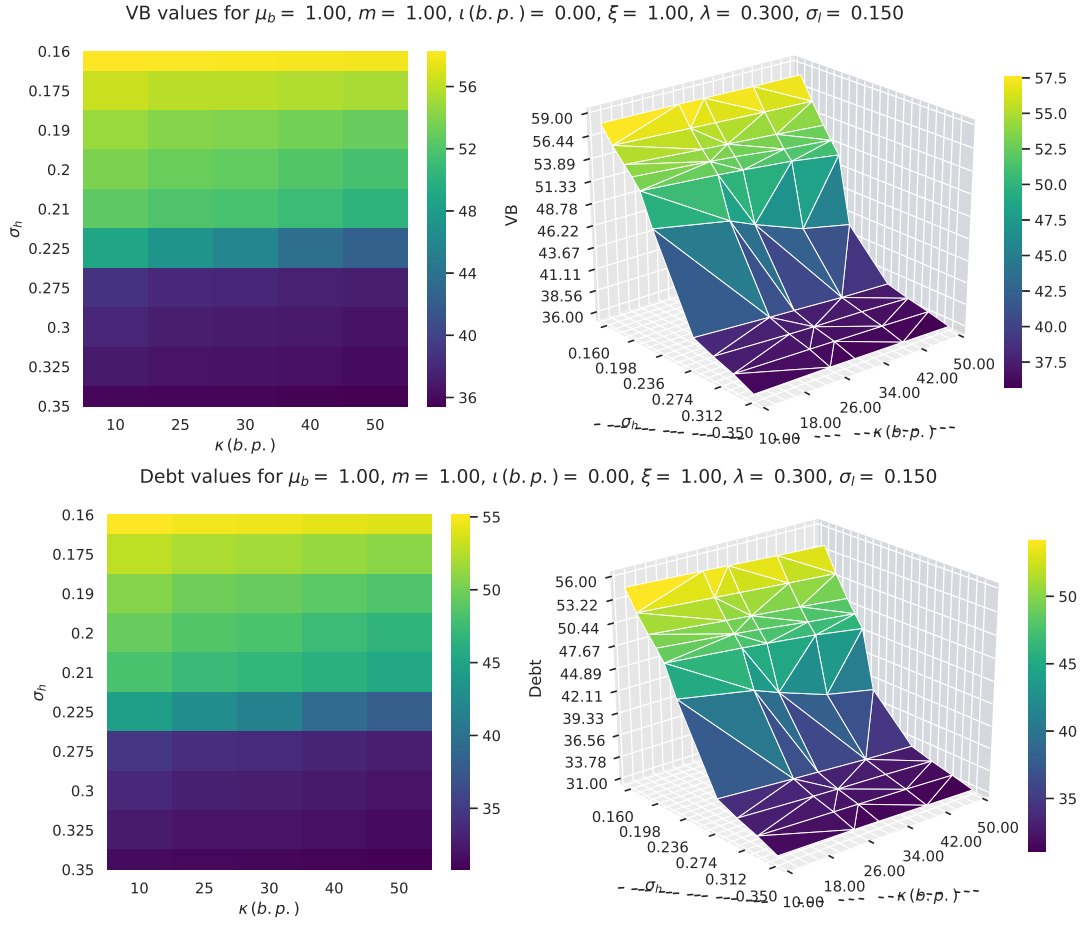
B.1.3 $\lambda = 0.30$

Figure 3. Model Results for $\lambda = 0.300$



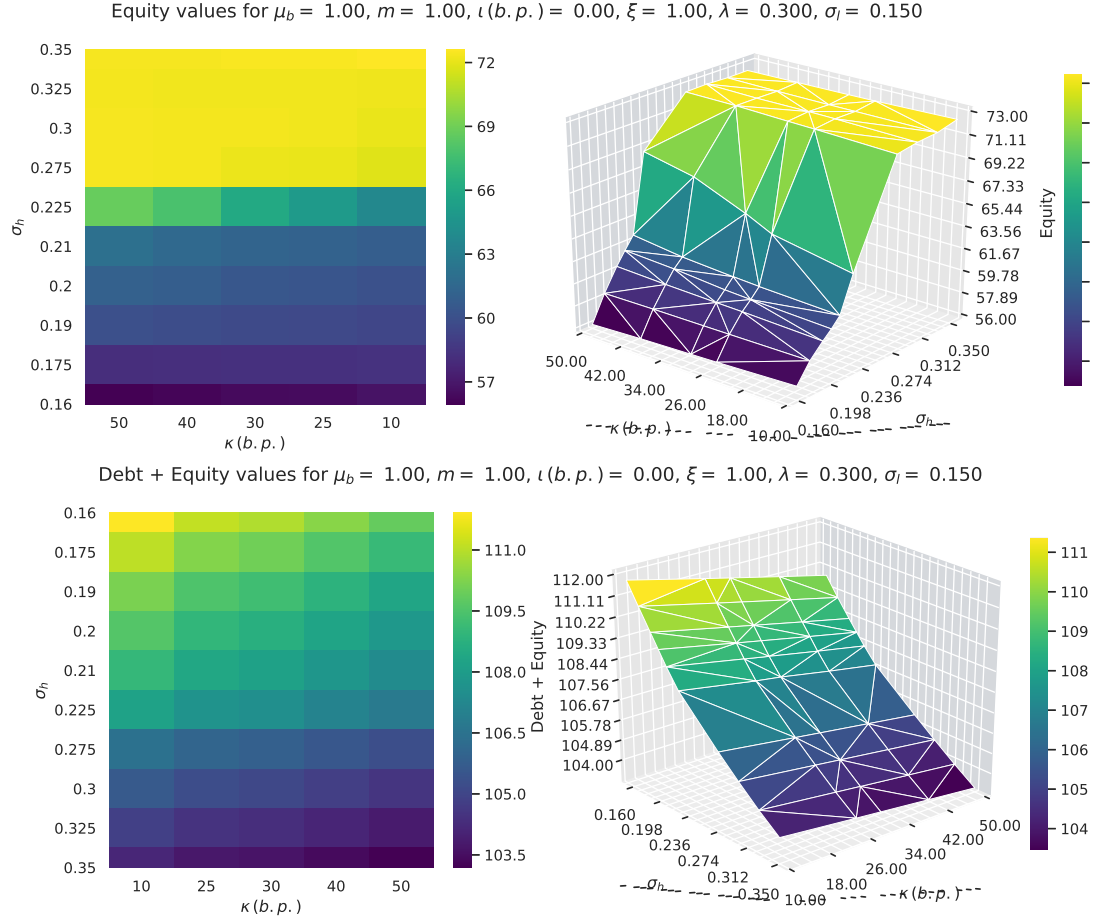
[Continues on the next page.]

Figure 3. Model Results for $\lambda = 0.300$



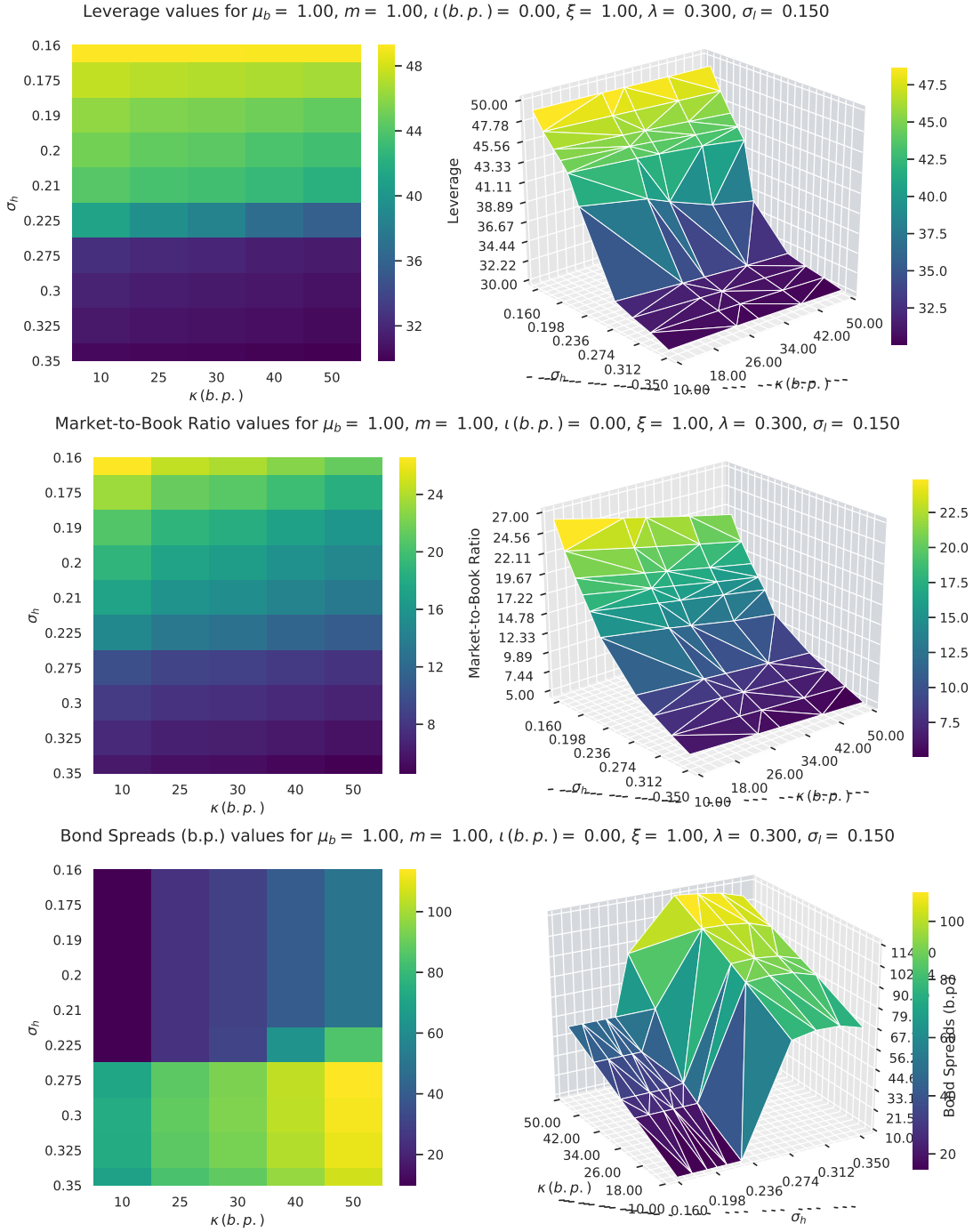
[Continues on the next page.]

Figure 3. Model Results for $\lambda = 0.300$



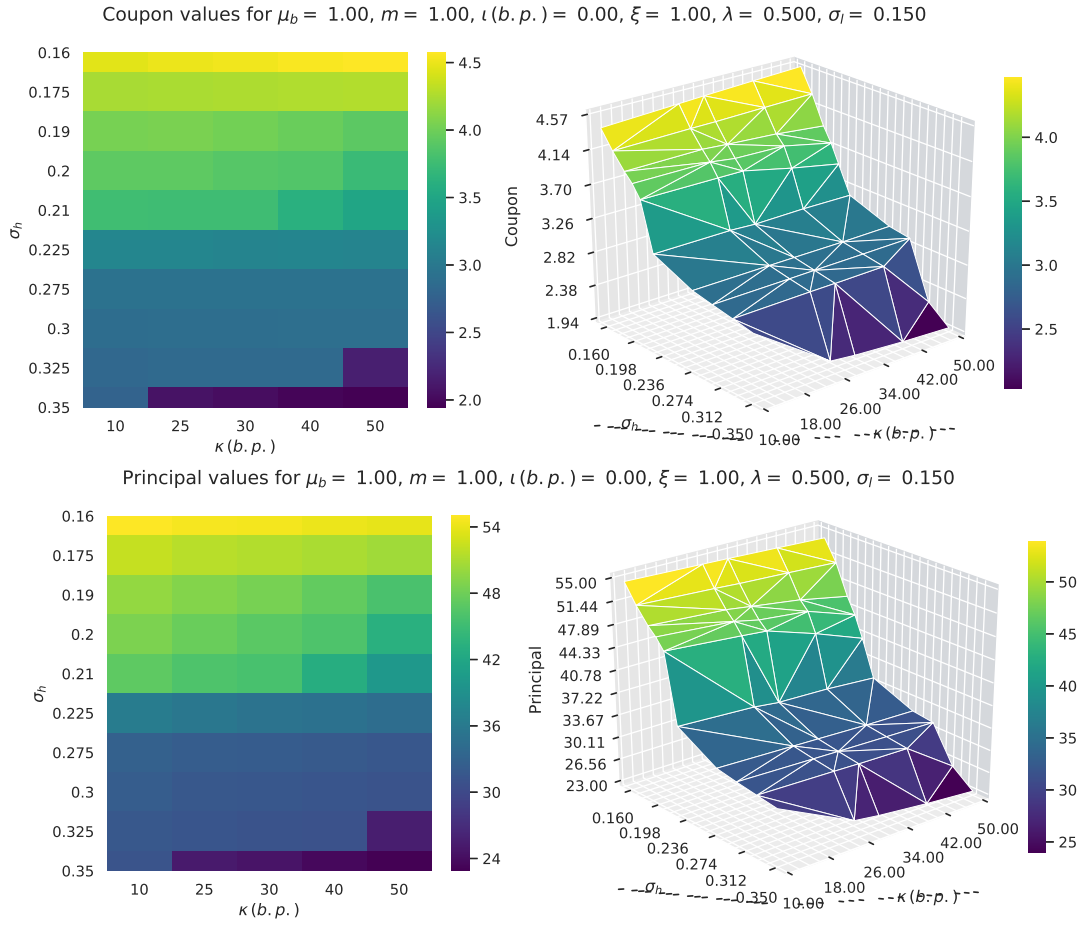
[Continues on the next page.]

Figure 3. Model Results for $\lambda = 0.300$



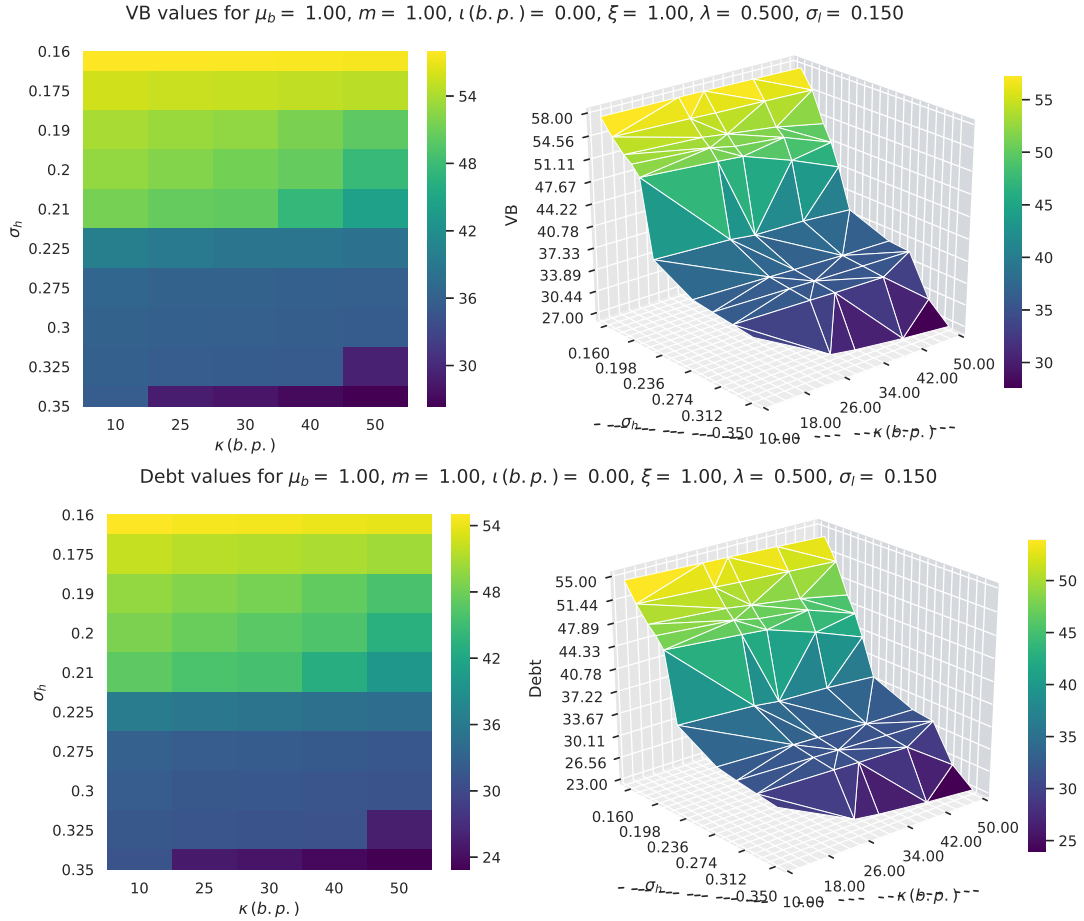
B.1.4 $\lambda = 0.50$

Figure 4. Model Results for $\lambda = 0.500$



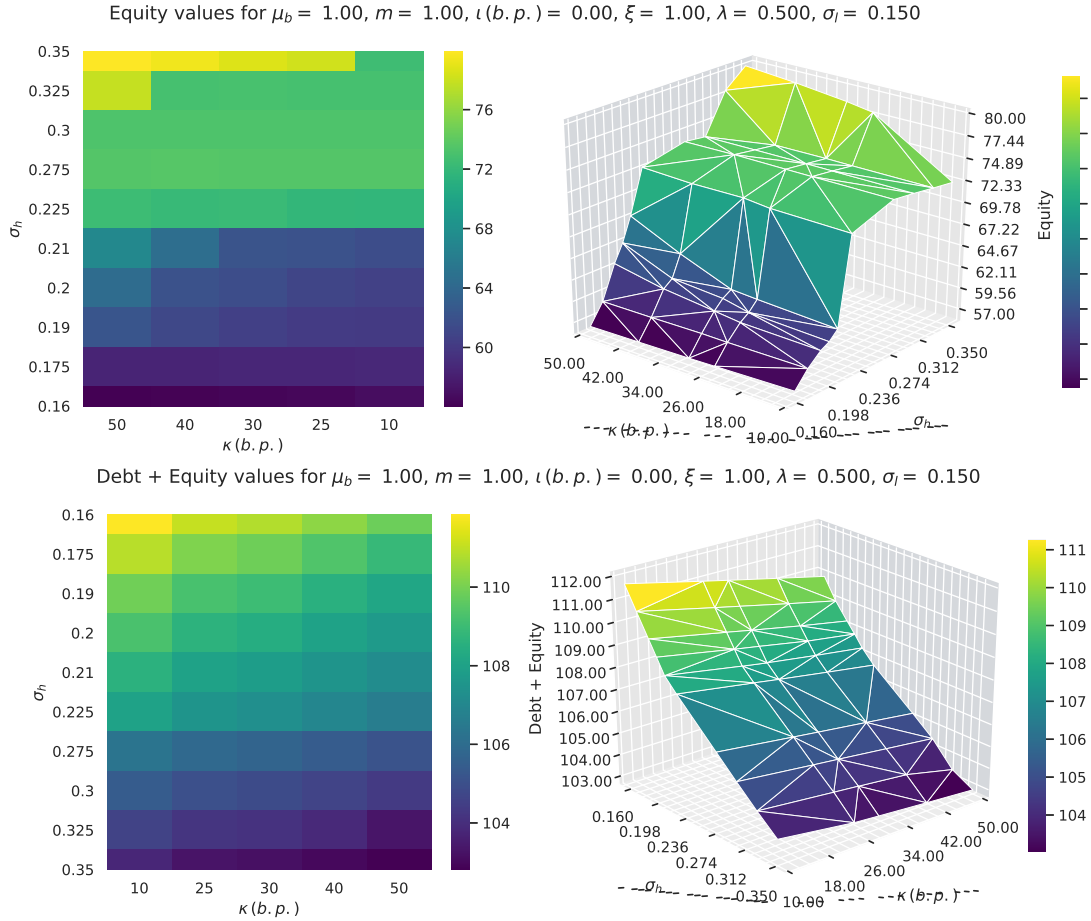
[Continues on the next page.]

Figure 4. Model Results for $\lambda = 0.500$



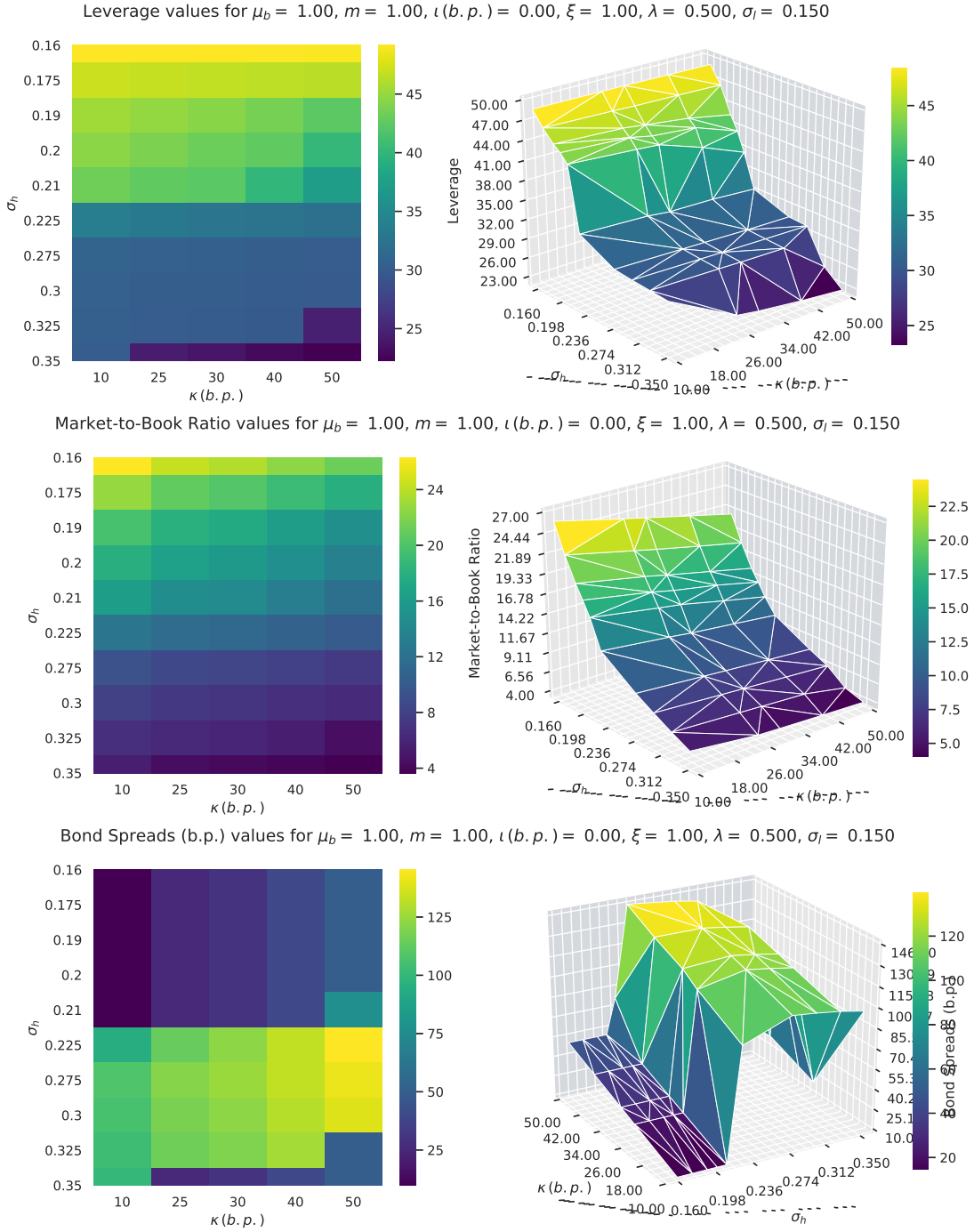
[Continues on the next page.]

Figure 4. Model Results for $\lambda = 0.500$



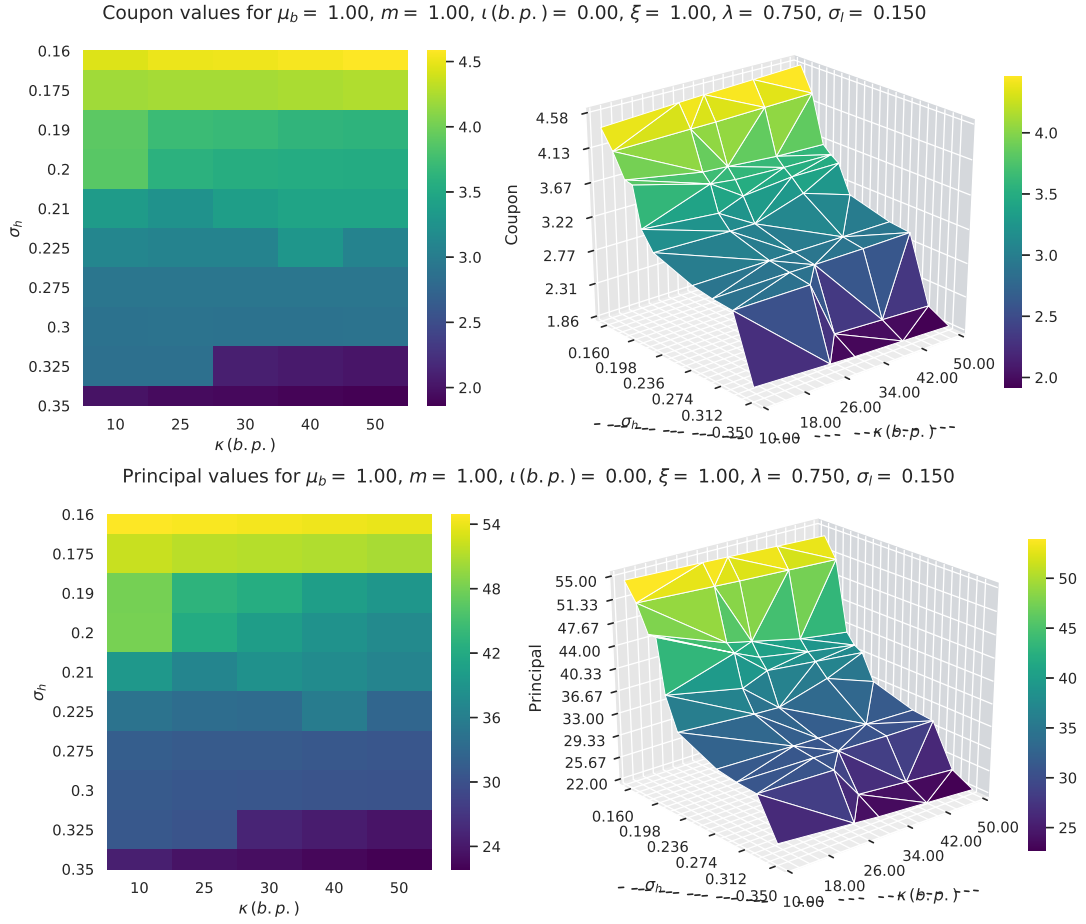
[Continues on the next page.]

Figure 4. Model Results for $\lambda = 0.500$



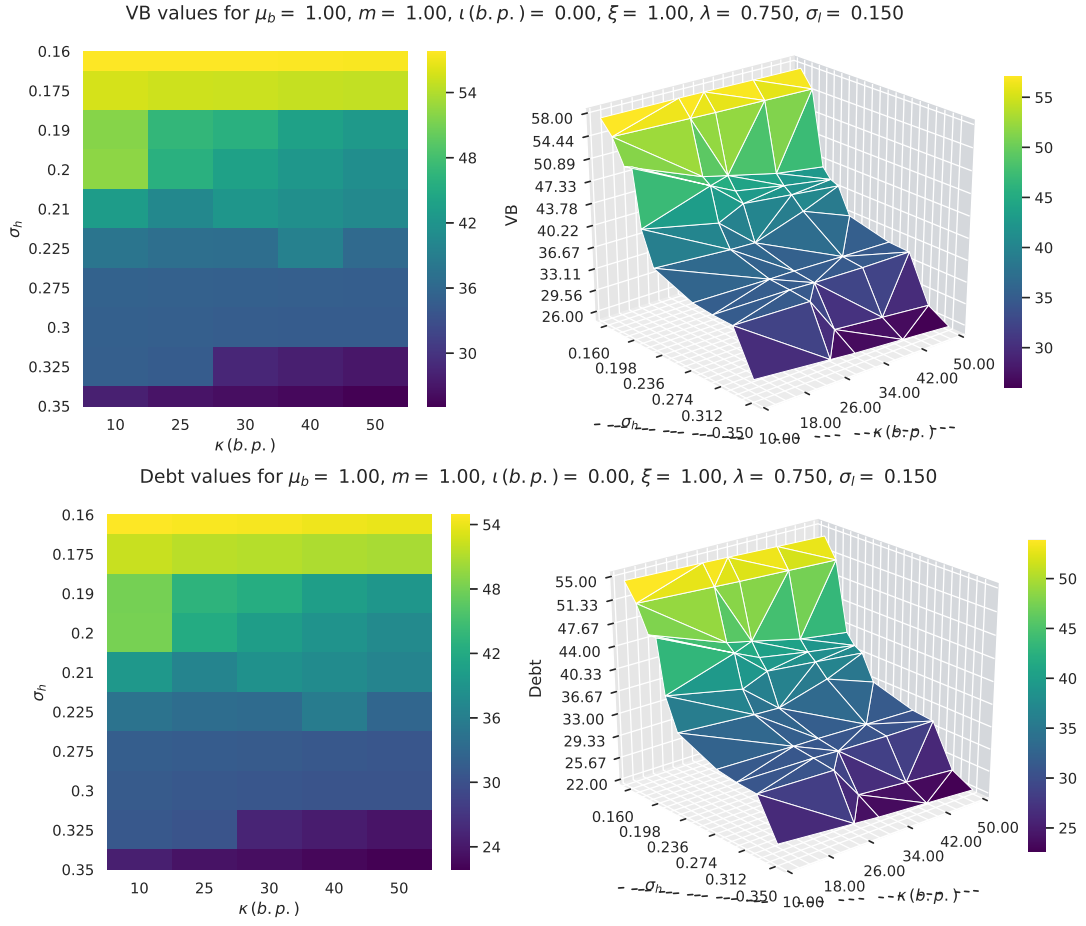
B.1.5 $\lambda = 0.75$

Figure 5. Model Results for $\lambda = 0.750$



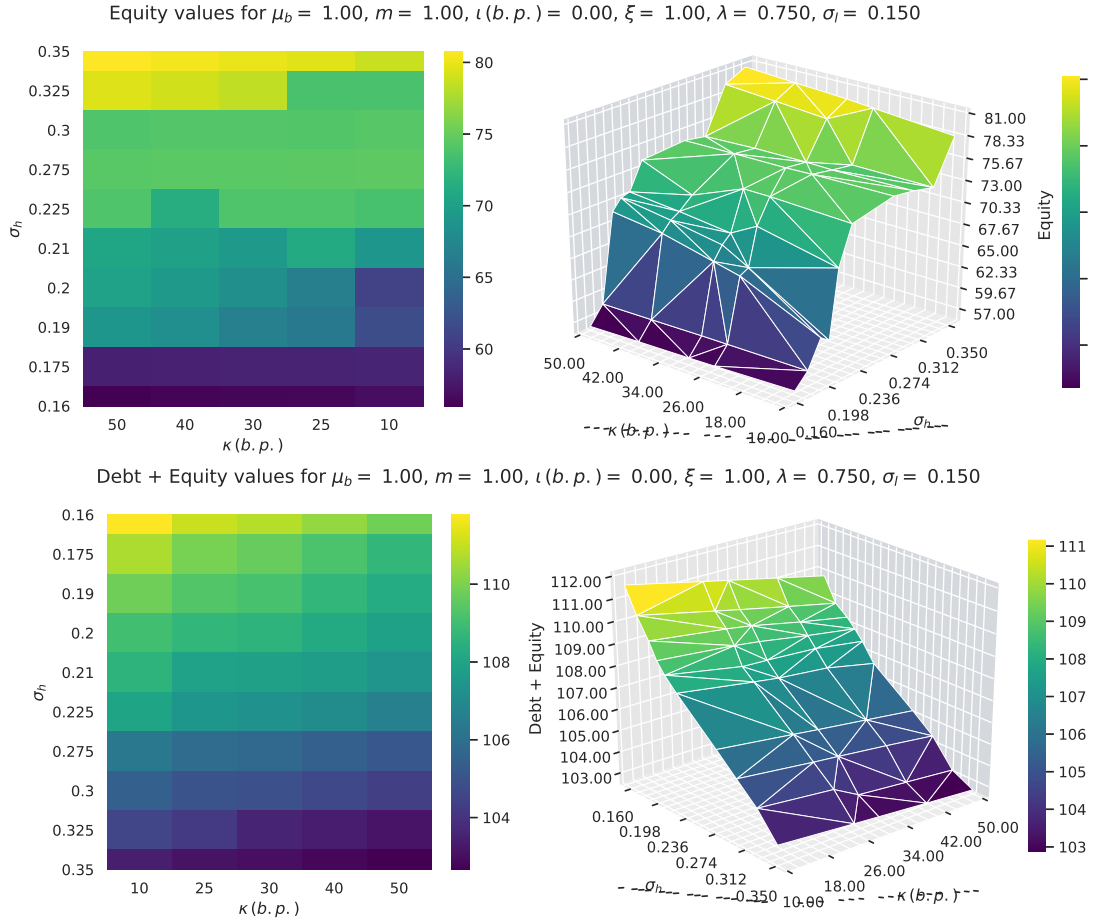
[Continues on the next page.]

Figure 5. Model Results for $\lambda = 0.750$



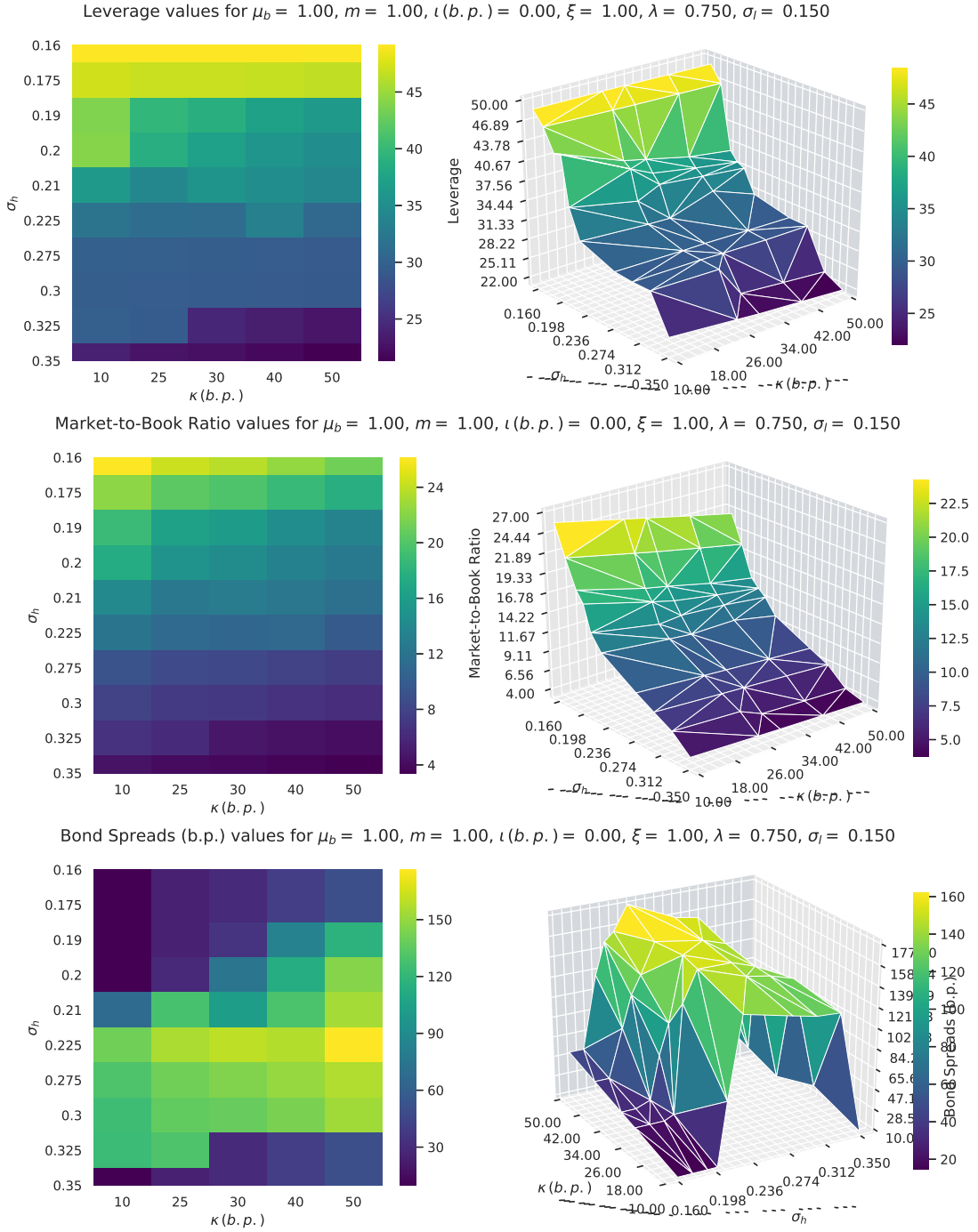
[Continues on the next page.]

Figure 5. Model Results for $\lambda = 0.750$



[Continues on the next page.]

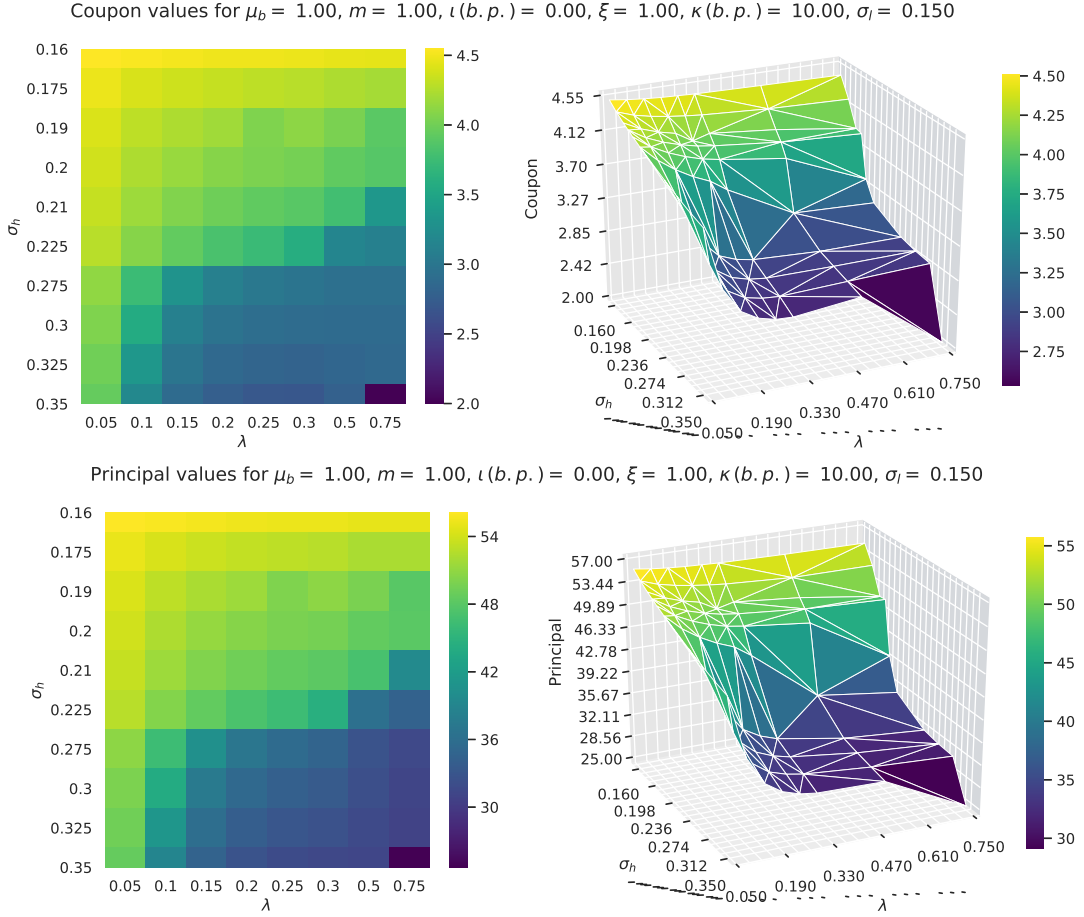
Figure 5. Model Results for $\lambda = 0.750$



B.2 Model Results for Varying κ Values in the $\lambda \times \sigma_h$ Plane

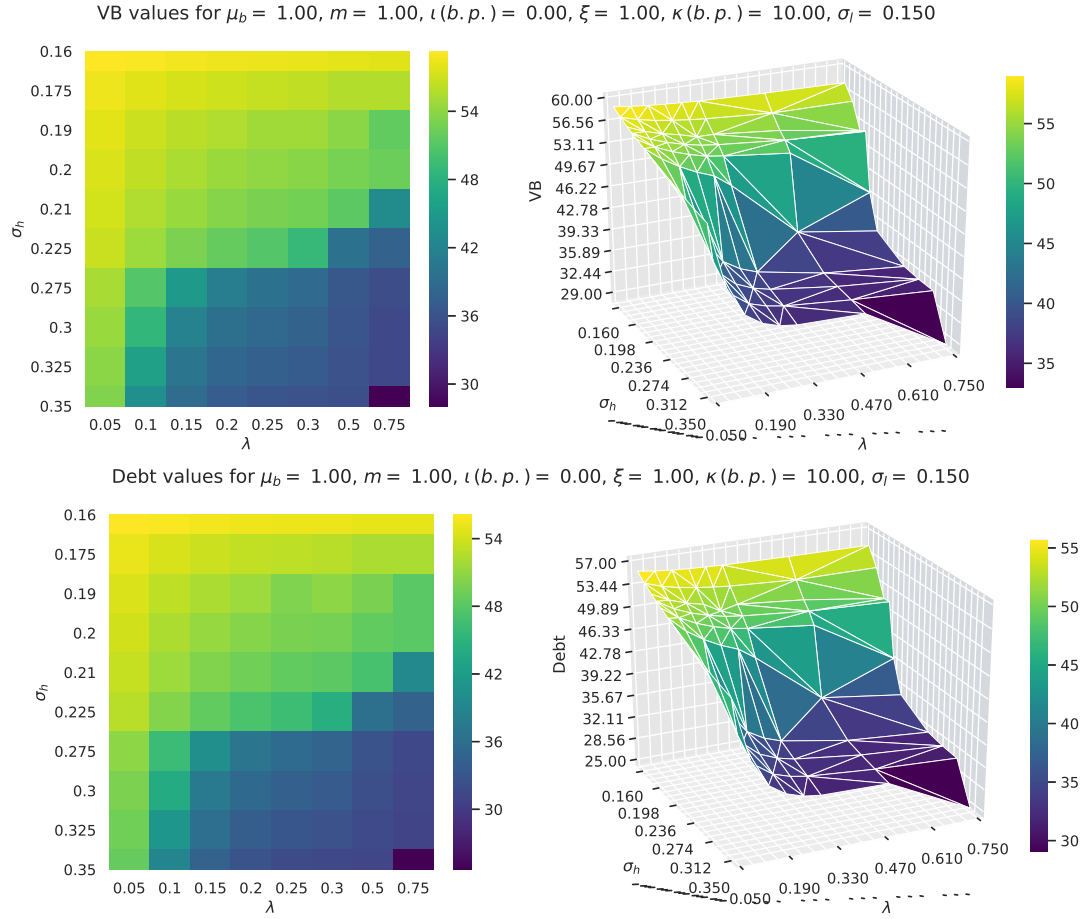
B.2.1 $\kappa^{EP} = 10$ (b.p.)

Figure 6. Model Results for $\kappa = 10.00$ (b.p.)



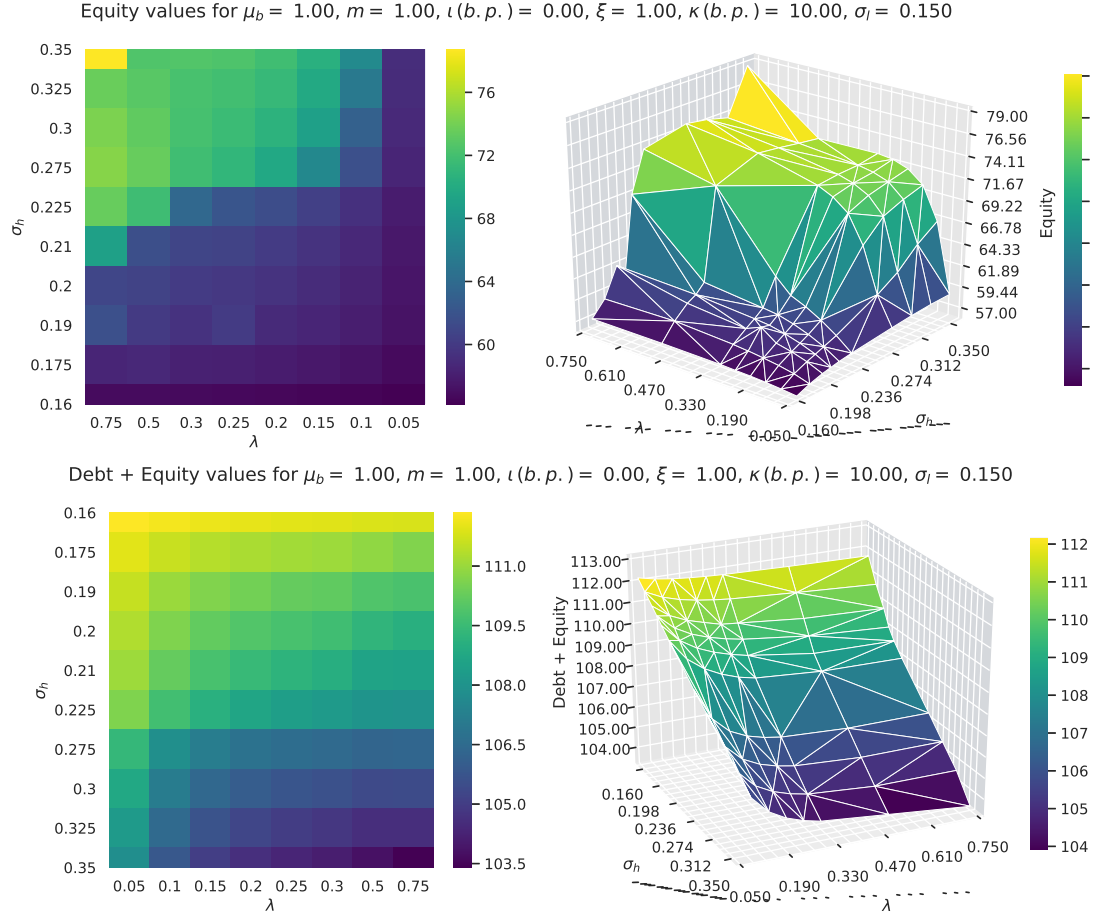
[Continues on the next page.]

Figure 6. Model Results for $\kappa = 10.00$ (b.p.)



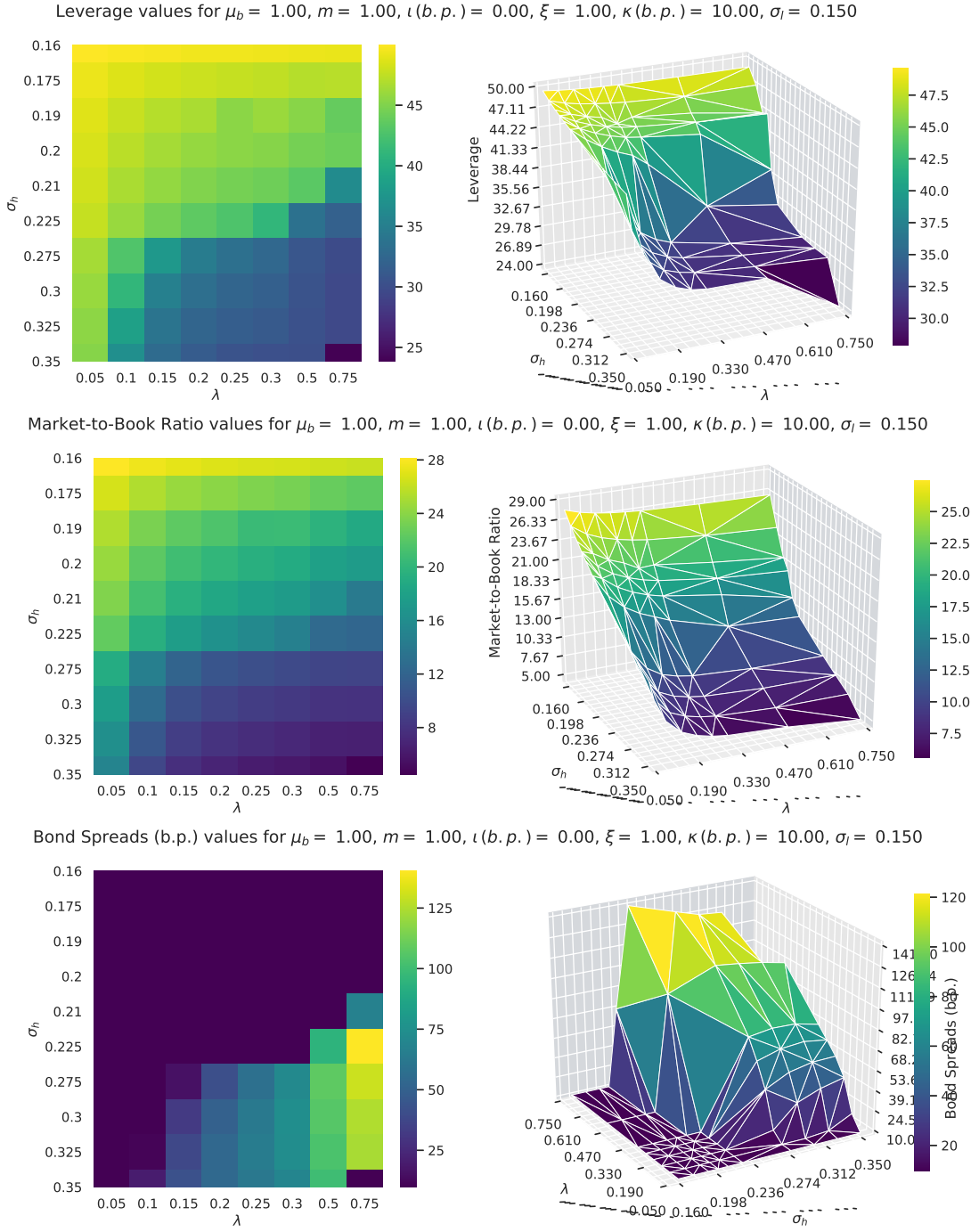
[Continues on the next page.]

Figure 6. Model Results for $\kappa = 10.00$ (b.p.)



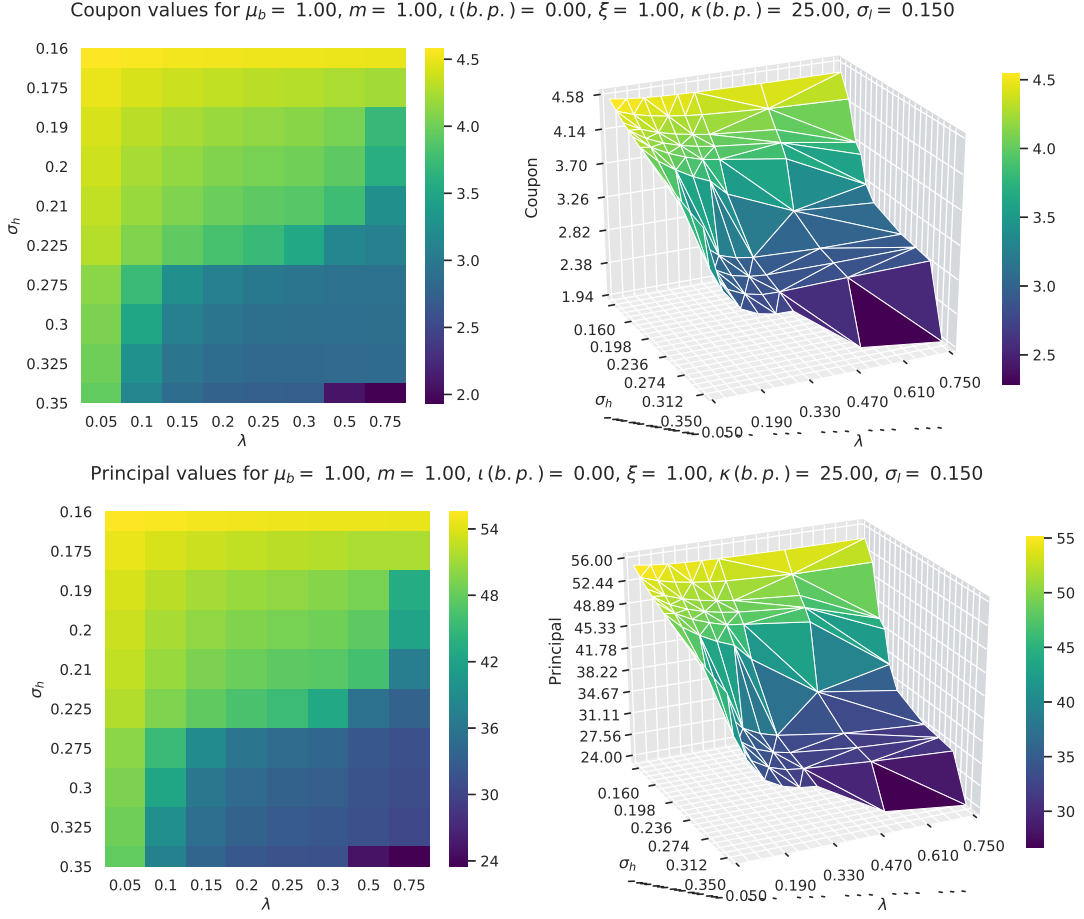
[Continues on the next page.]

Figure 6. Model Results for $\kappa = 10.00$ (b.p.)



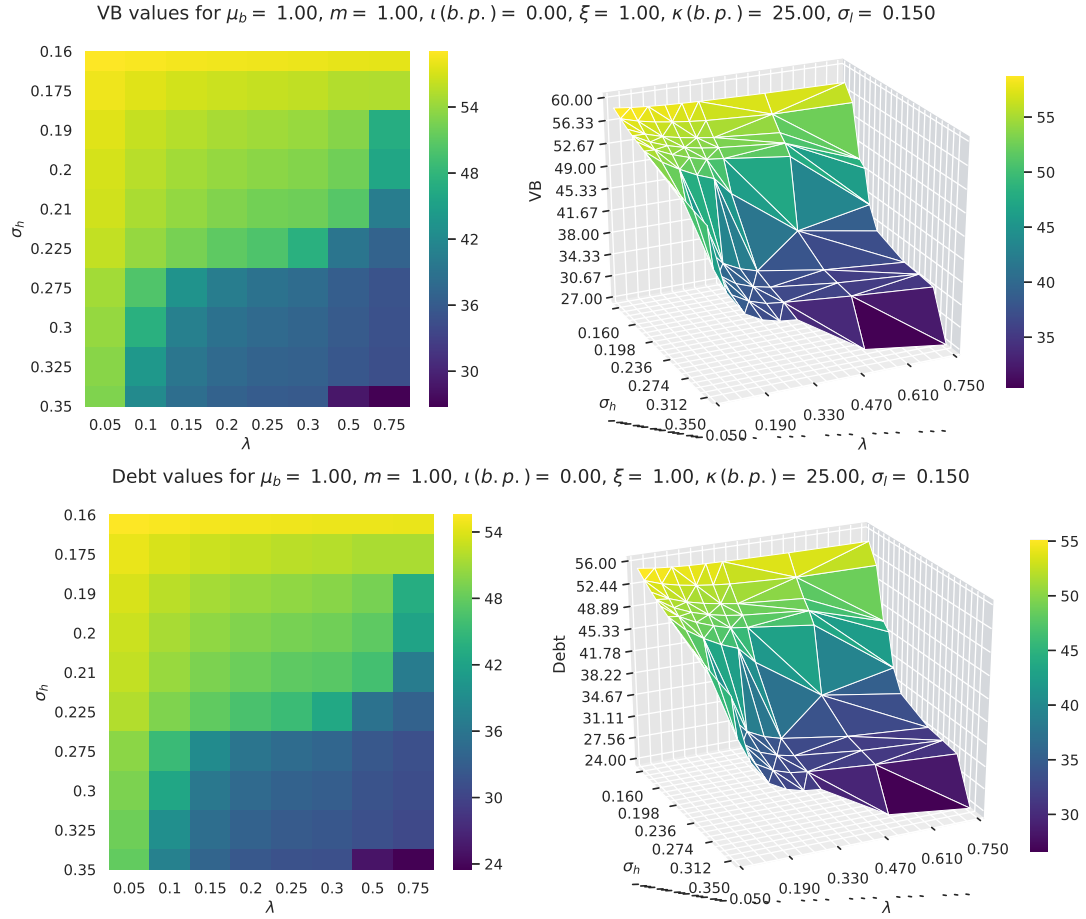
B.2.2 $\kappa^{EP} = 25$ (b.p.)

Figure 7. Model Results for $\kappa = 25.00$ (b.p.)



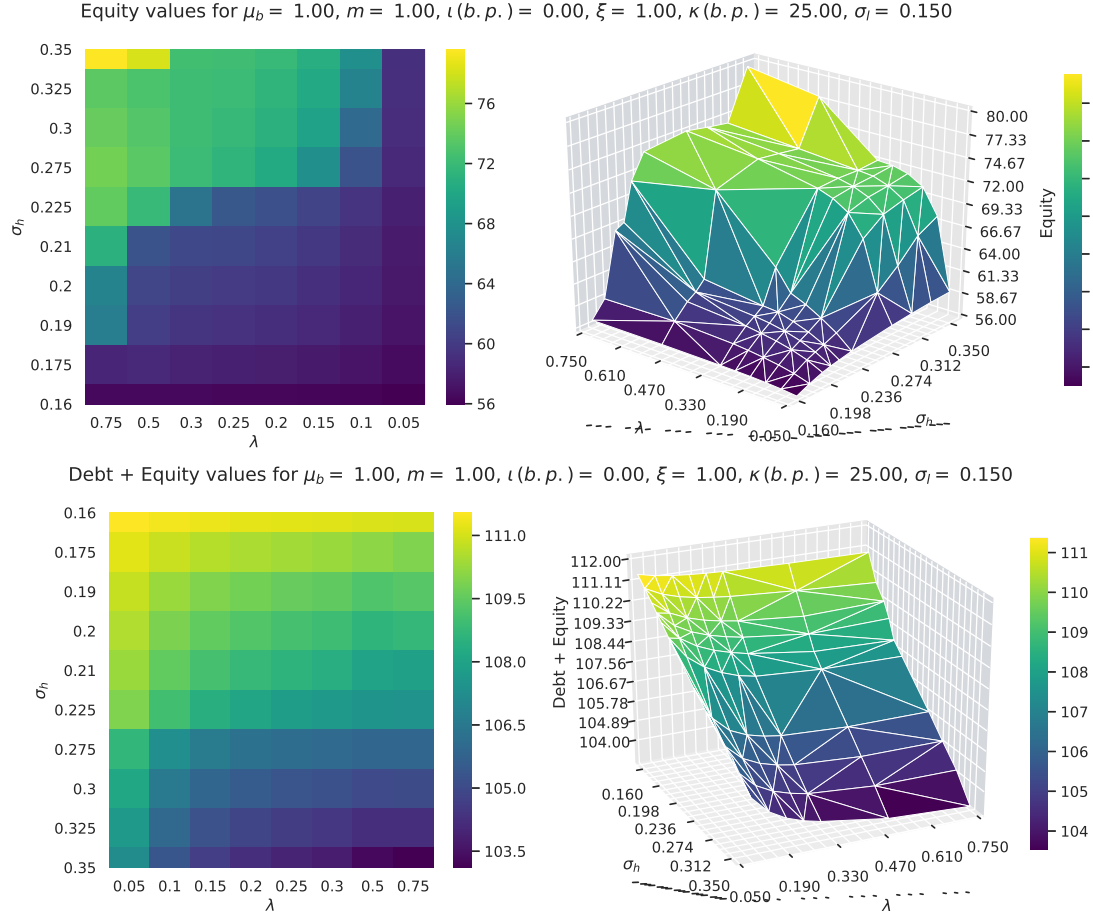
[Continues on the next page.]

Figure 7. Model Results for $\kappa = 25.00$ (b.p.)



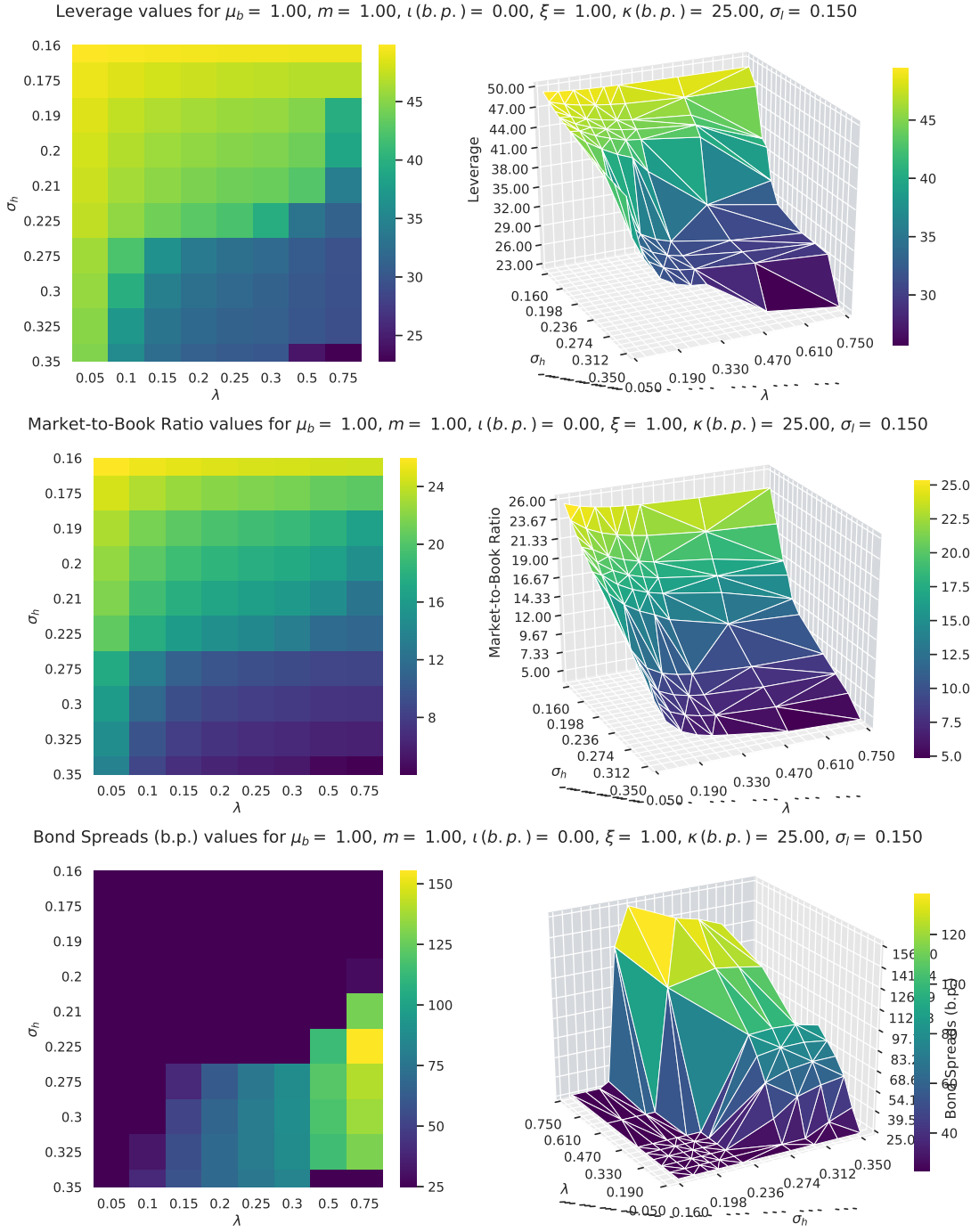
[Continues on the next page.]

Figure 7. Model Results for $\kappa = 25.00$ (b.p.)



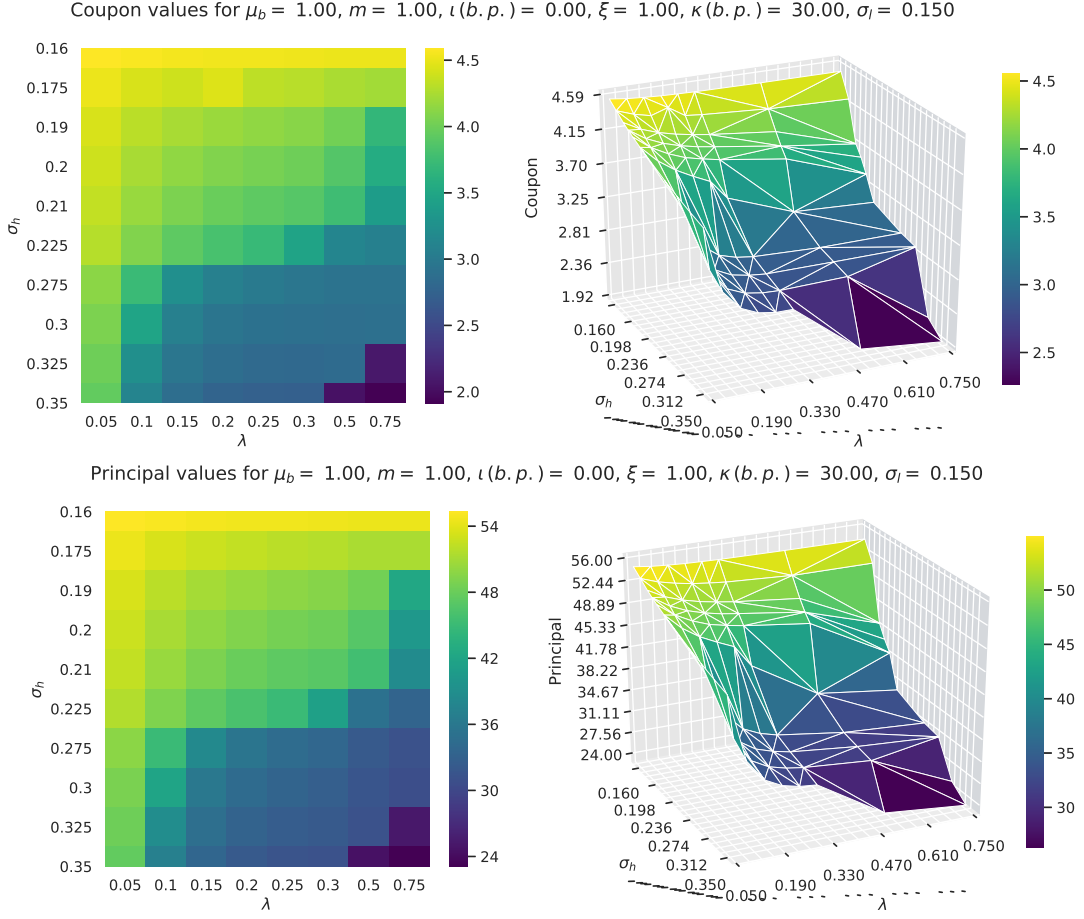
[Continues on the next page.]

Figure 7. Model Results for $\kappa = 25.00$ (b.p.)



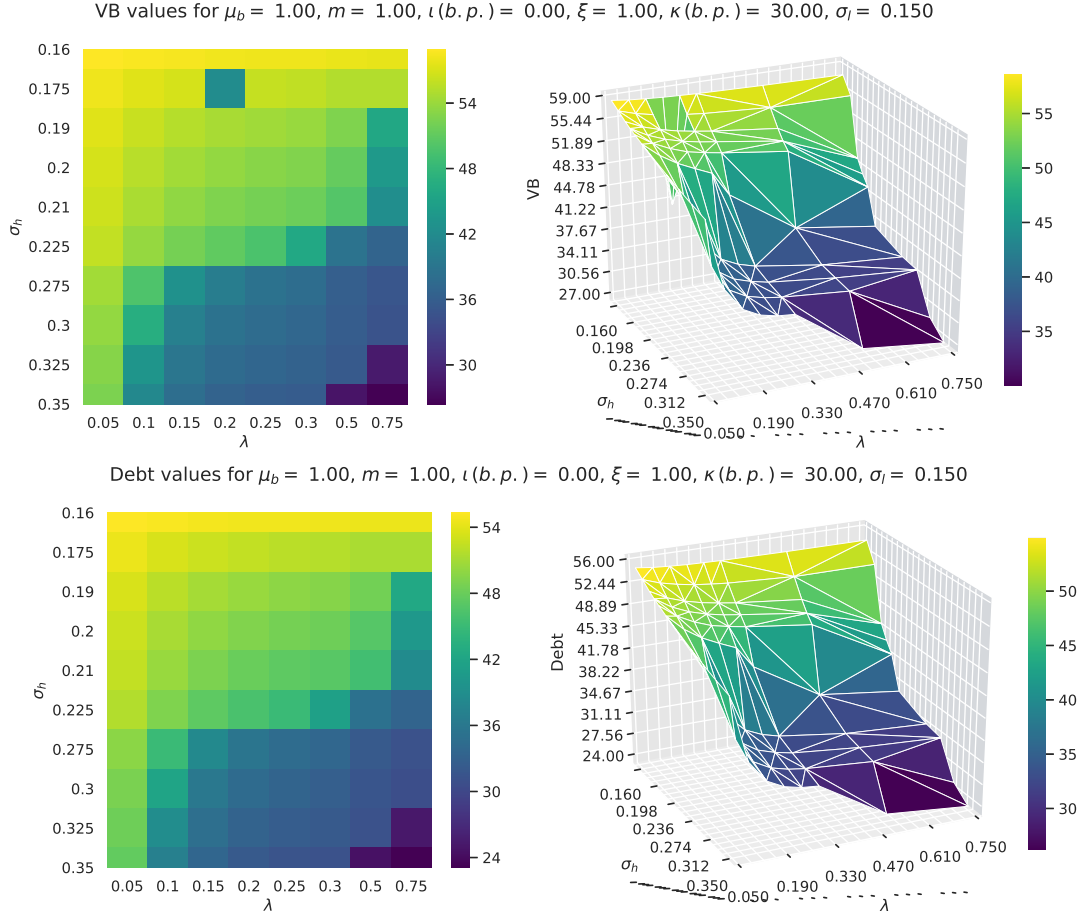
B.2.3 $\kappa^{EP} = 30$ (b.p.)

Figure 8. Model Results for $\kappa = 30.00$ (b.p.)



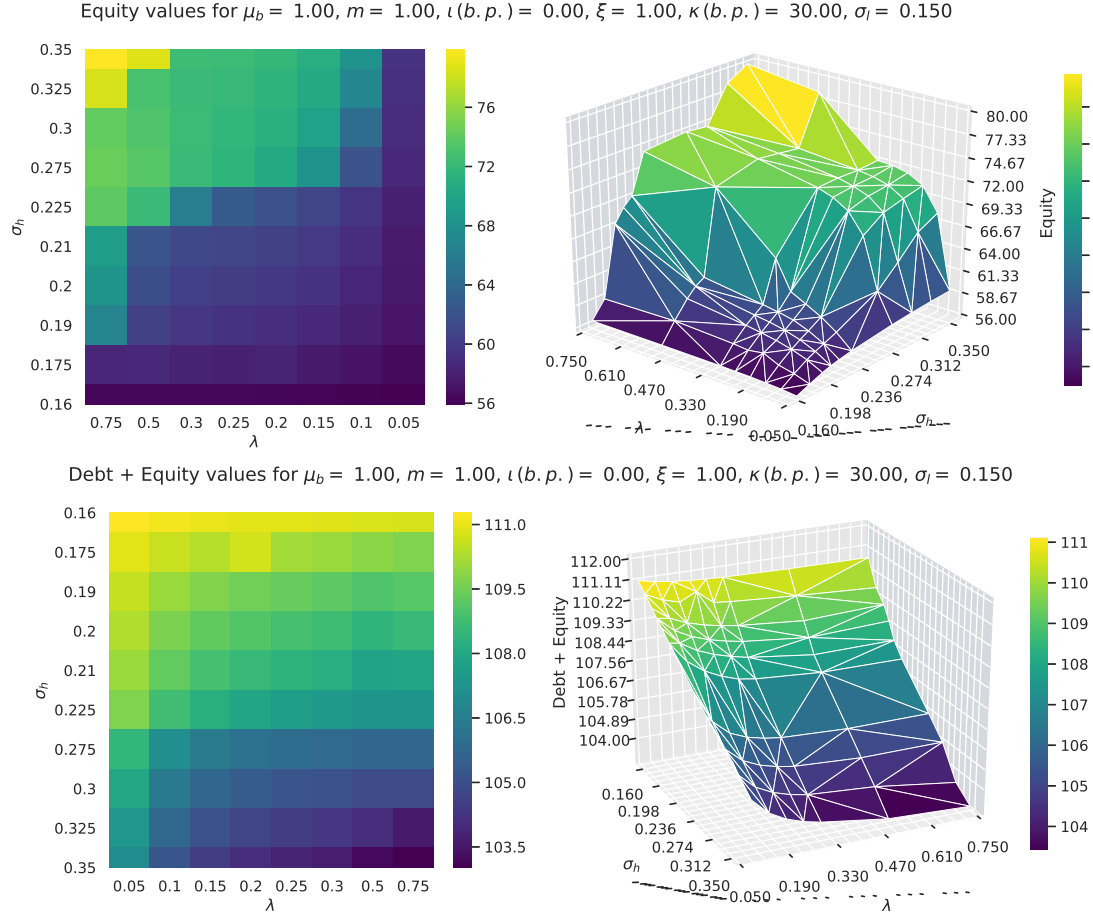
[Continues on the next page.]

Figure 8. Model Results for $\kappa = 30.00$ (b.p.)



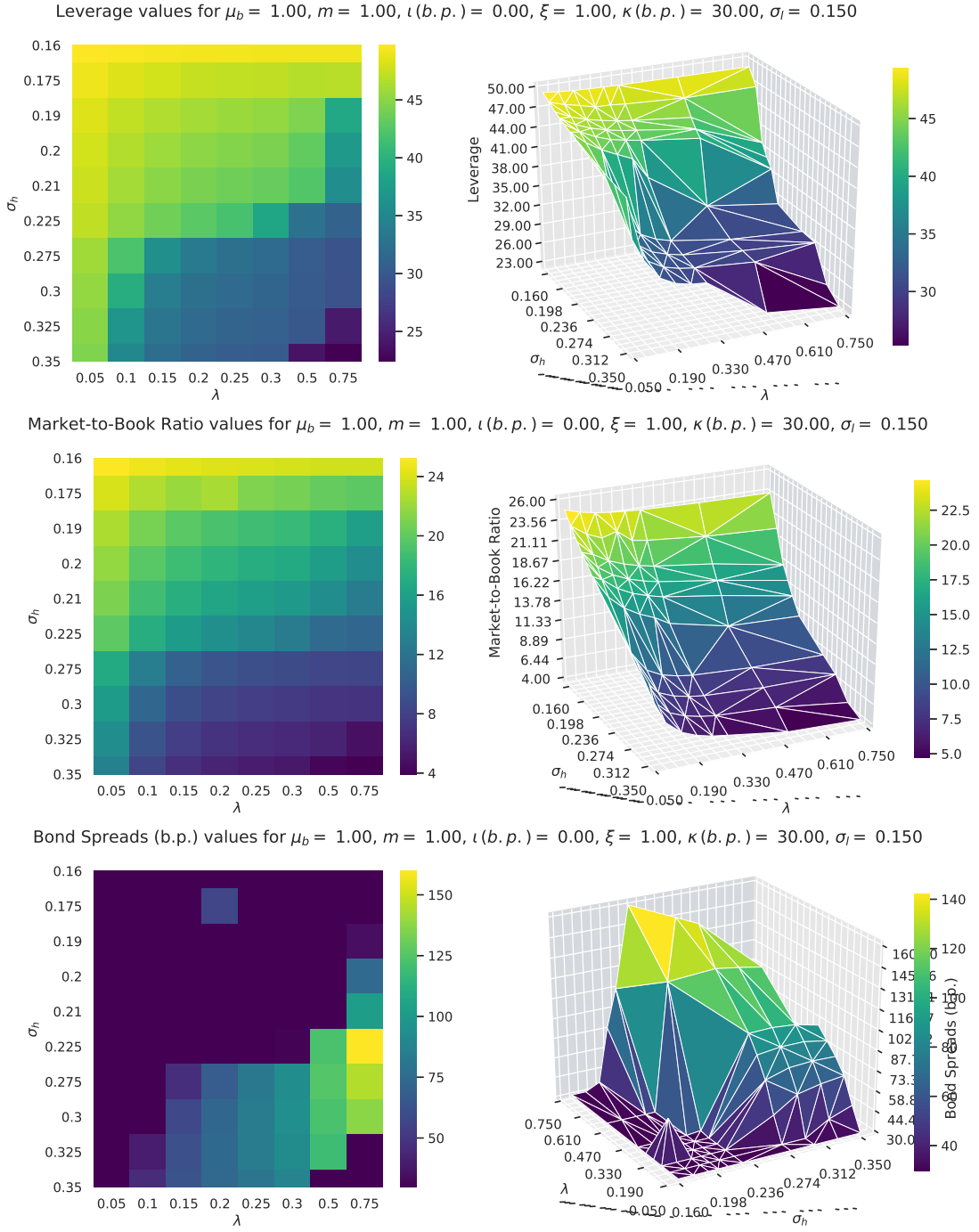
[Continues on the next page.]

Figure 8. Model Results for $\kappa = 30.00$ (b.p.)



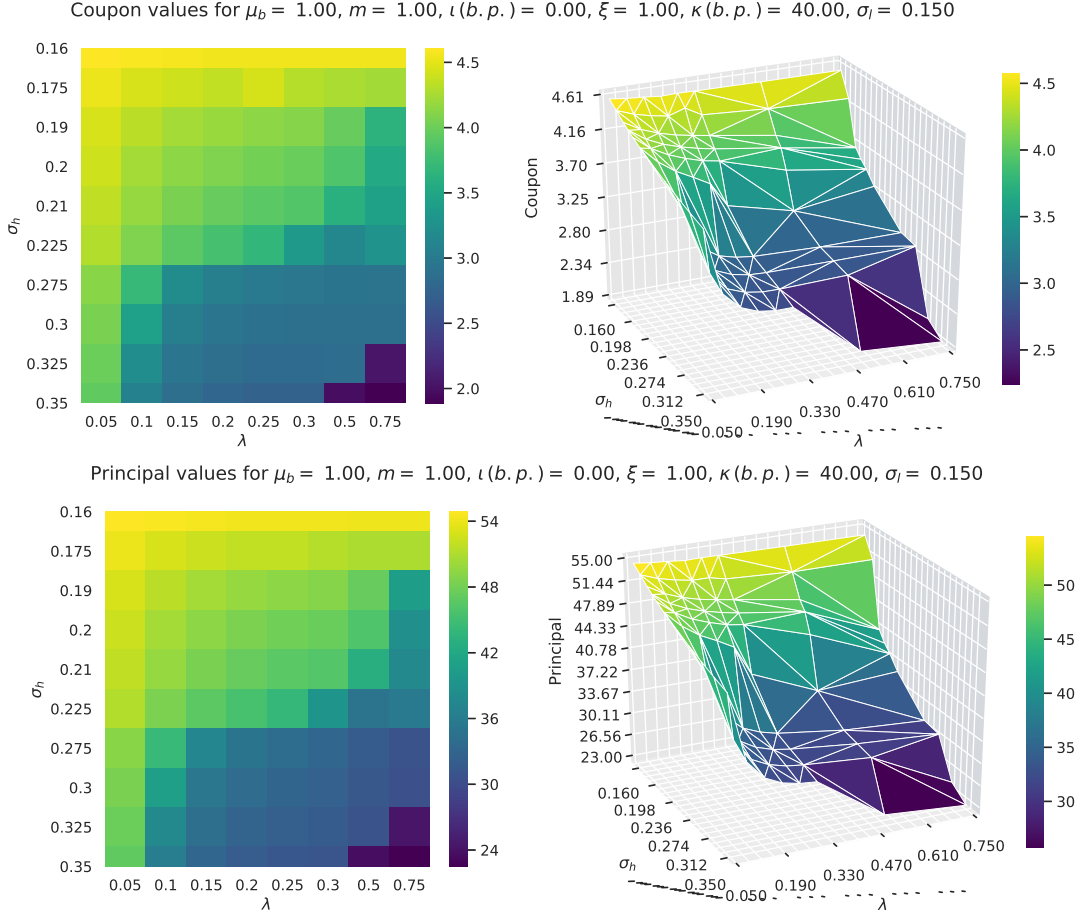
[Continues on the next page.]

Figure 8. Model Results for $\kappa = 30.00$ (b.p.)



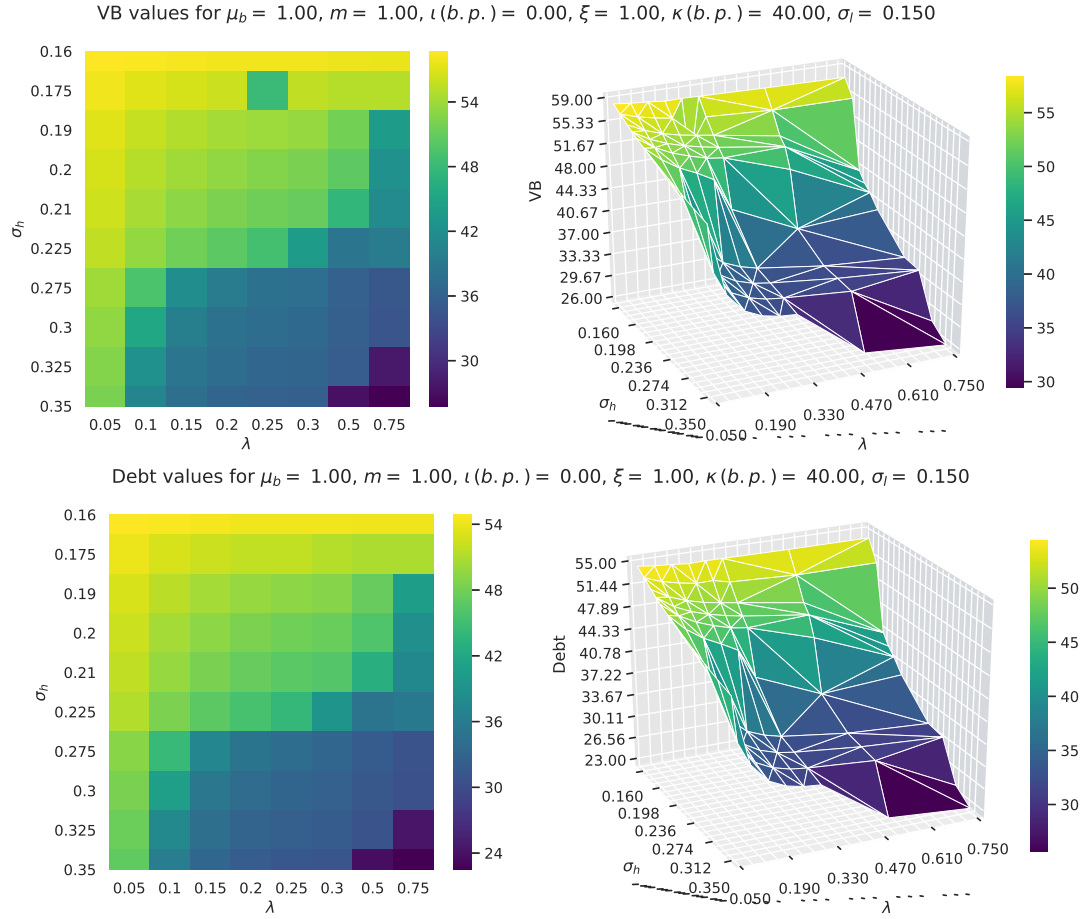
B.2.4 $\kappa^{EP} = 40$ (b.p.)

Figure 9. Model Results for $\kappa = 40.00$ (b.p.)



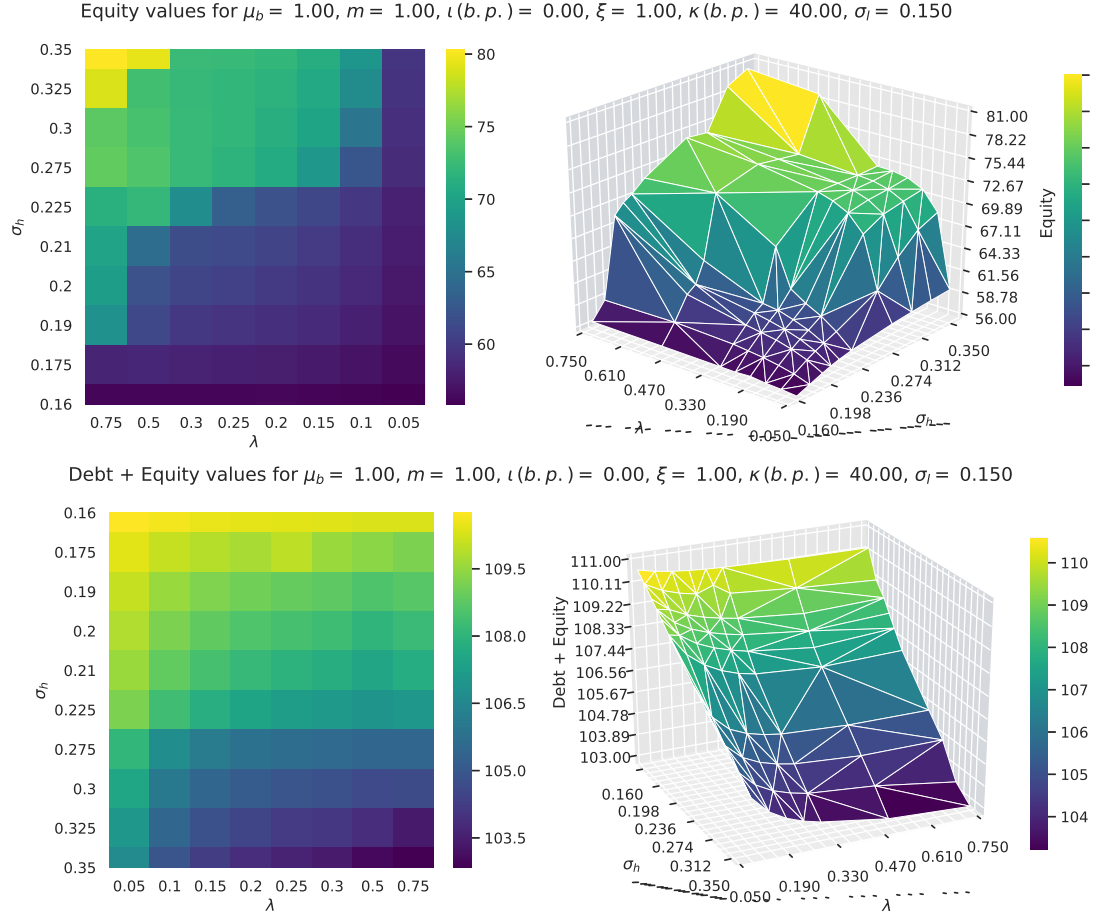
[Continues on the next page.]

Figure 9. Model Results for $\kappa = 40.00$ (b.p.)



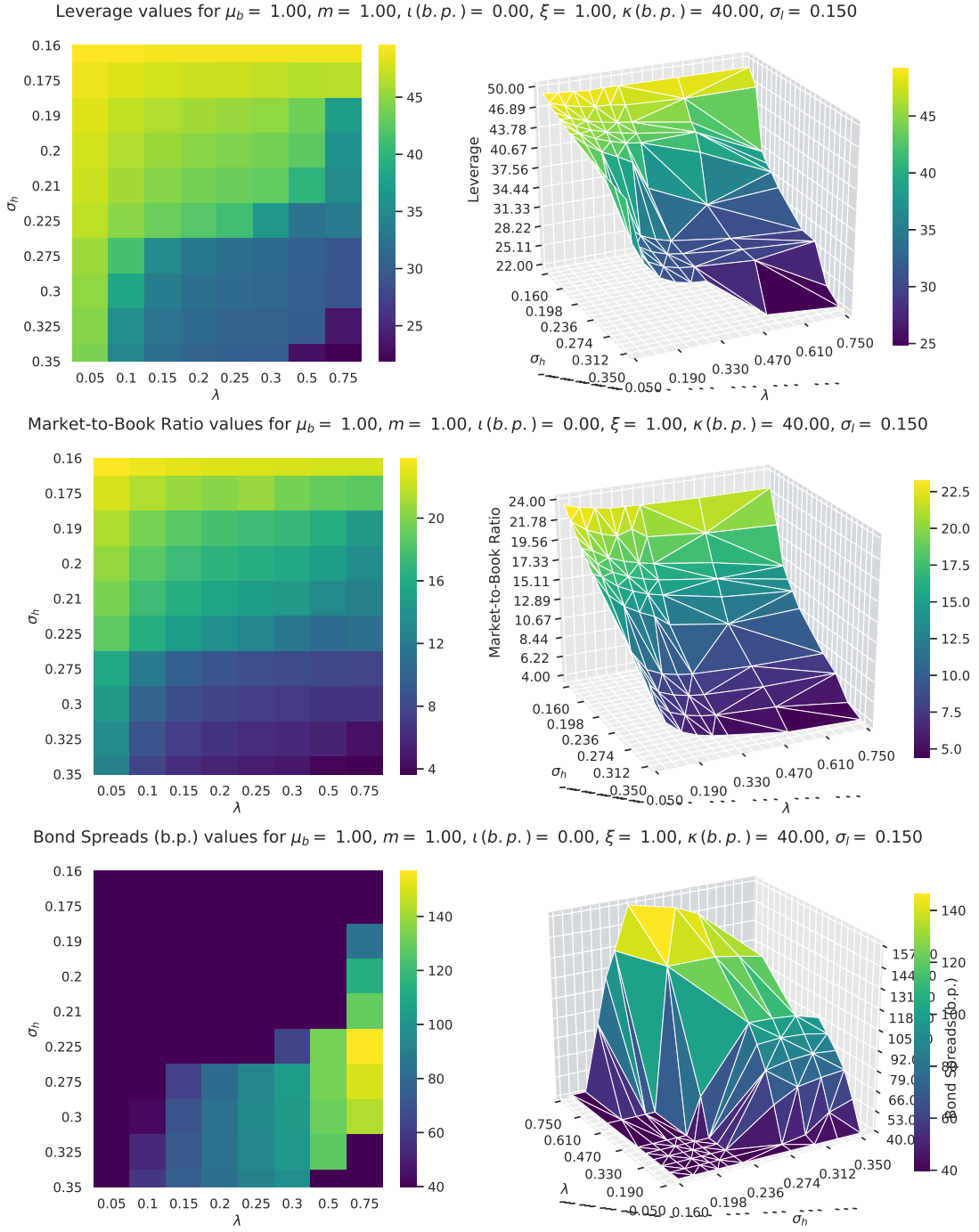
[Continues on the next page.]

Figure 9. Model Results for $\kappa = 40.00$ (b.p.)



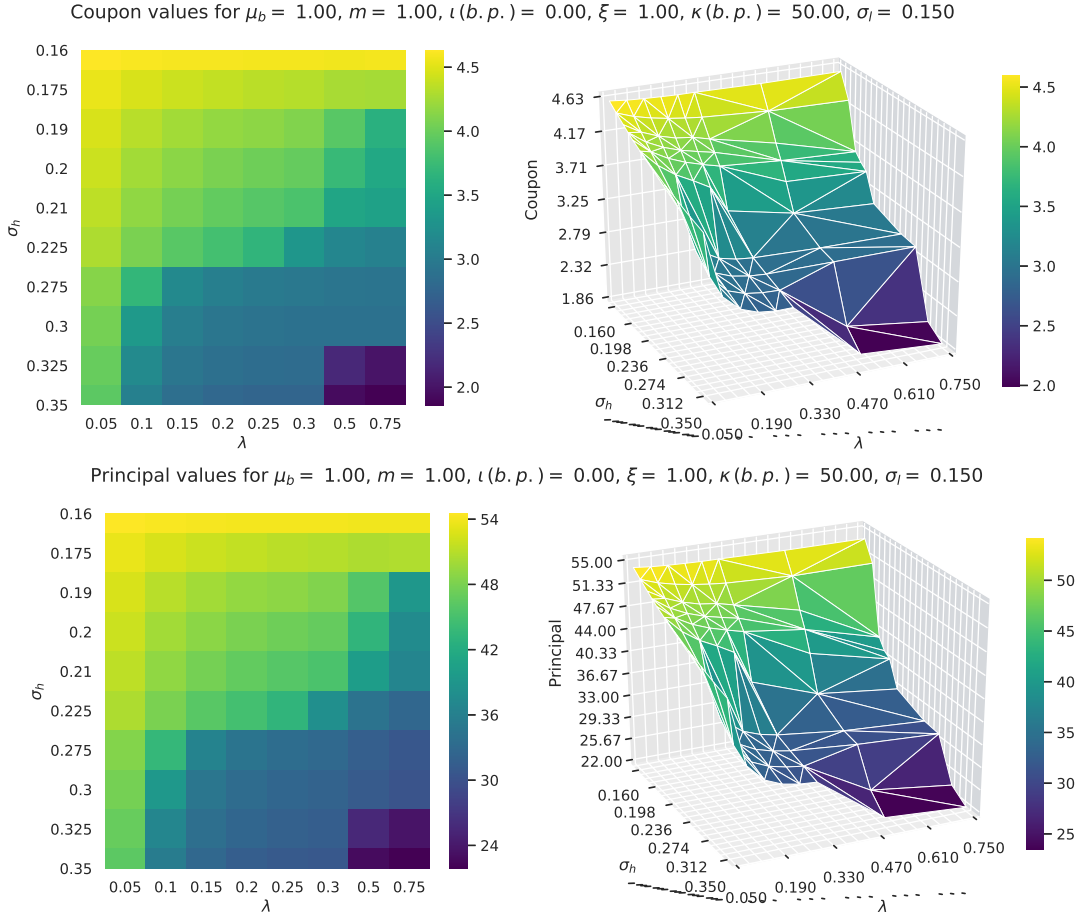
[Continues on the next page.]

Figure 9. Model Results for $\kappa = 40.00$ (b.p.)



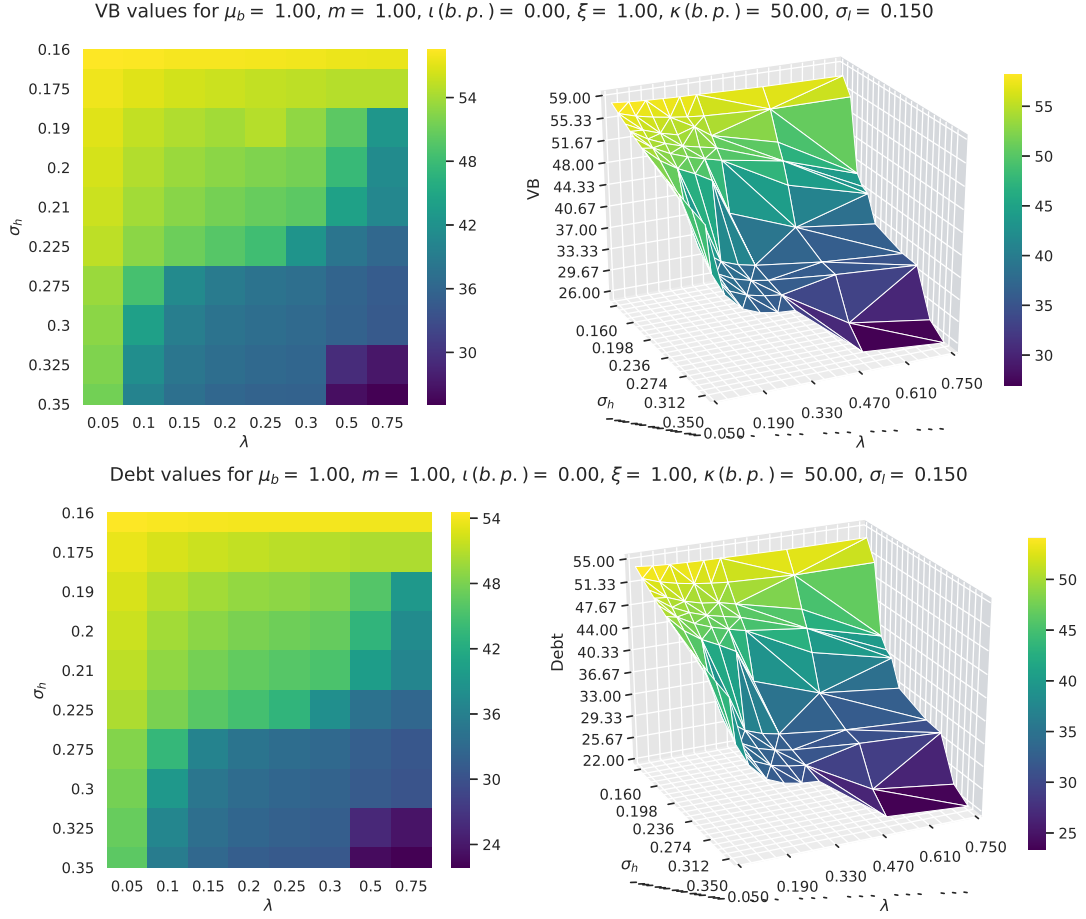
B.2.5 $\kappa^{EP} = 50$ (b.p.)

Figure 10. Model Results for $\kappa = 50.00$ (b.p.)



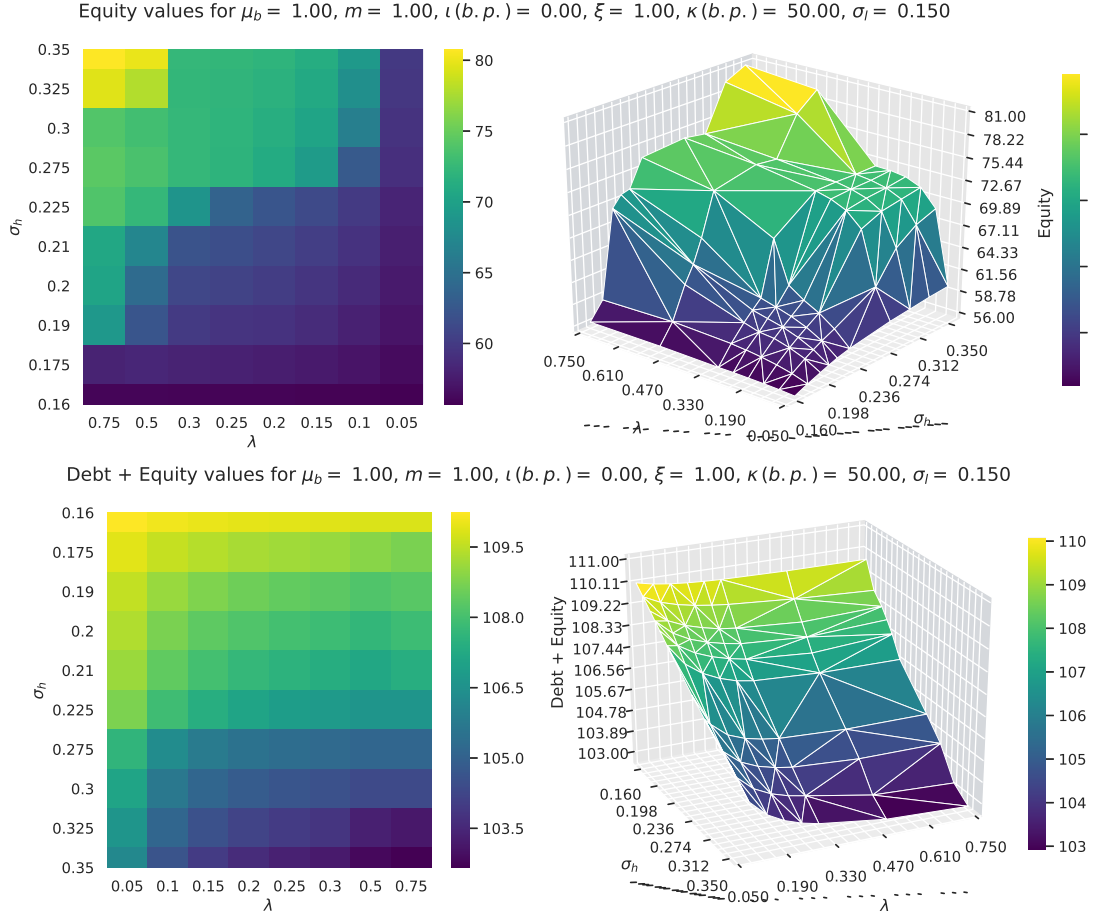
[Continues on the next page.]

Figure 10. Model Results for $\kappa = 50.00$ (b.p.)



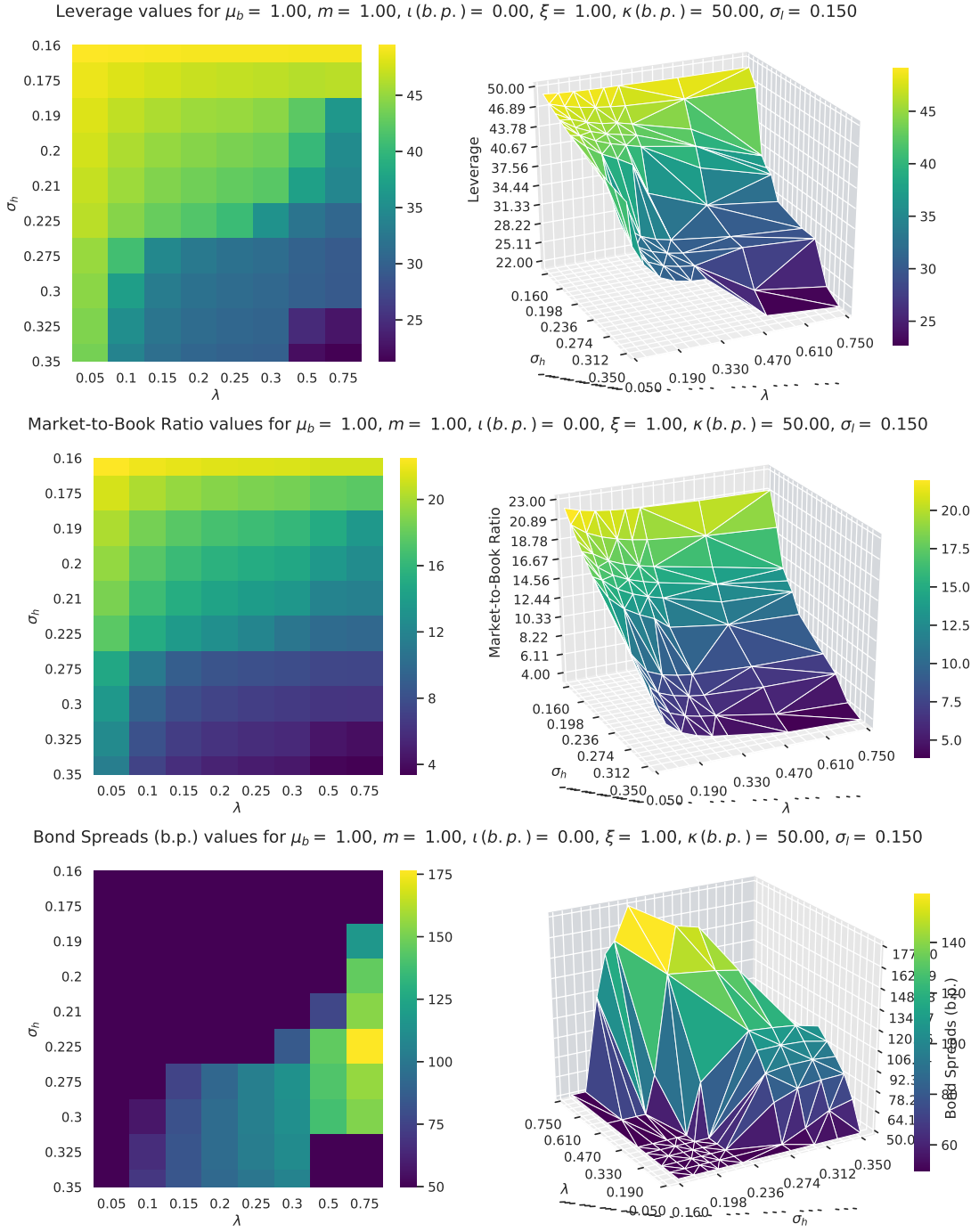
[Continues on the next page.]

Figure 10. Model Results for $\kappa = 50.00$ (b.p.)



[Continues on the next page.]

Figure 10. Model Results for $\kappa = 50.00$ (b.p.)



Appendix C. Interpolating the Pre-Volatility Shock Bond Pricing Formula

This section describes a numerical approach for the computation of the pre-volatility-shock bond price. It consists on expressing this pricing formula as a sum of simple functions that are independent of the bond coupon c and principal p . I start by recalling the SVM bond price function in Theorem ??:

$$\begin{aligned} d(V_t, \tau; V_l^B, \lambda, \omega, \theta) &= \frac{c}{r_{disc} + \lambda} + e^{-(r_{disc} + \lambda)\tau} \left[p - \frac{c}{r_{disc} + \lambda} \right] \left[1 - F\left(\tau, \ln\left(\frac{V_t}{V_l^B}\right); \sigma_l\right) \right] \\ &+ \left[\frac{\alpha V_l^B}{\mu_b \cdot m} - \frac{c}{r_{disc} + \lambda} \right] G\left(\tau, \ln\left(\frac{V_t}{V_l^B}\right); \theta_l\right) \\ &+ \lambda \int_t^{t+\tau} e^{-(r_{disc} + \lambda)(s-t)} \left\{ \int_{V_l^B}^\infty d_{\bar{\sigma}}(V, \tau - s; V_{\bar{\sigma}}^B(\omega, \theta_h), \omega, \theta_h) \times \right. \\ &\quad \times \left[-\frac{\partial}{\partial V} \Psi^{v, td}\left(s - t, \ln\left(\frac{V}{V_l^B}\right); \ln\left(\frac{V_t}{V_l^B}\right), \sigma_l\right) \right] dV \Big\} \cdot ds \end{aligned}$$

for $V_l^B \in (0, V_0)$, where $\omega \equiv (\mu_b, m, c, p)$, $\theta \equiv (r_{grow}, r_{disc}, \sigma_l, \sigma_h)$, $\theta_j \equiv (r_{disc}, r_{grow}, \sigma_j)$, $j = l, h$, $r_{disc} \equiv r + \xi\kappa$, $r_{grow} \equiv r - \bar{\delta}$,

$$\Psi^{v, td}(u, \bar{v}; v, \sigma) \equiv N\left(\frac{-\bar{v} + v + \hat{a}(\sigma)\sigma^2 u}{\sigma\sqrt{u}}\right) - e^{-2\hat{a}(\sigma)v} N\left(\frac{-\bar{v} - v + \hat{a}(\sigma)\sigma^2 u}{\sigma\sqrt{u}}\right)$$

$V_{\bar{\sigma}}^B(\omega, \theta_h)$ is the optimal post-shock default barrier established in Theorem ??, and the functions \hat{a} , \hat{z} , F , G and the CVM bond price $d_{\bar{\sigma}}(\cdot; \cdot)$ are as defined in Theorem ??:

$$d_{\bar{\sigma}}(V_t, \tau; V^B, \omega, \theta_h) = \frac{c}{r_{disc}} + e^{-r_{disc}\tau} \left[p - \frac{c}{r_{disc}} \right] (1 - F(\tau, v_t; \theta_0)) + \left[\frac{\alpha V^B}{\mu_b \cdot m} - \frac{c}{r_{disc}} \right] G(\tau, v_t; \theta_h)$$

where $\theta_0 \equiv (r_{grow}, \sigma)$,

$$\begin{aligned} F(u, v_t; \theta_0) &= N(h_1(u, v_t; \theta_0)) + e^{-2\hat{a}v_t} N(h_2(u, v_t; \theta_0)) \\ G(u, v_t; \theta) &= e^{\{\hat{z}(\theta) - \hat{a}(\theta_0)\}v_t} N(q_1(u, v_t; \theta)) + e^{-\{\hat{z}(\theta) + \hat{a}(\theta_0)\}v_t} N(q_2(u, v_t; \theta)) \\ h_1(u, v_t; \theta_0) &= \frac{(-v_t - \hat{a}(\theta_0)\sigma^2 u)}{\sigma\sqrt{u}}, \quad h_2(u, v_t; \theta_0) = \frac{(-v_t + \hat{a}(\theta_0)\sigma^2 u)}{\sigma\sqrt{u}} \\ q_1(u, v_t; \theta) &= \frac{(-v_t - \hat{z}(\theta)\sigma^2 u)}{\sigma\sqrt{u}}, \quad q_2(u, v_t; \theta) = \frac{(-v_t + \hat{z}(\theta)\sigma^2 u)}{\sigma\sqrt{u}} \\ v_t &\equiv \ln\left(\frac{V_t}{V^B}\right), \quad \hat{a}(\theta_0) \equiv \frac{r_{grow} - \frac{1}{2}\sigma^2}{\sigma^2}, \quad \hat{z}(\theta) \equiv \frac{[\hat{a}(\theta_0)^2\sigma^4 + 2r_{disc}\sigma^2]^{1/2}}{\sigma^2} \end{aligned}$$

and $N(\cdot)$ is the cumulative standard normal distribution.

C.1 The SVM Bond Price Inner Integral

I focus on the integral on the RHS of the pre-volatility shock bond pricing formula:

$$J(V, \tau; V^B, \omega, \lambda, \theta) = \lambda \int_t^{t+\tau} e^{-(r_{disc} + \lambda)(s-t)} \left\{ \int_{V^B}^\infty d_{\bar{\sigma}}(V, \tau - s; V_{\bar{\sigma}}^B(\omega, \theta_h), \omega, \theta_h) \times \right.$$

$$\times \left[-\frac{\partial}{\partial V} \Psi^{v,t^d}(s-t, v(V; V^B); v(V_t; V^B), \sigma_l) \right] dV \Big\} \cdot ds \quad (C1)$$

By Claim ?? in Appendix ??[correct reference](#), the value of the post-volatility-shock bond price converges to that of a credit-risk-free bond as $V \rightarrow \infty$.

$$\lim_{V \uparrow \infty} d_{\bar{\sigma}}(V_t, \tau; V^B, \omega, \theta) = b^{crf}(\tau; r_{disc}, \omega)$$

where

$$\begin{aligned} b^{crf}(\tau; r_{disc}, \omega) &\equiv \int_t^{t+\tau} e^{-r_{disc} \cdot (s-t)} c \cdot ds + e^{-r_{disc} \cdot \tau} p \\ &= \frac{c}{r_{disc}} + e^{-r_{disc} \cdot \tau} \left(p - \frac{c}{r_{disc}} \right) \end{aligned} \quad (C2)$$

Let V^{max} be the smallest value of V for which

$$b^{crf}(\tau; r_{disc}, \omega) - \min\{d_{\bar{\sigma}}(V_t, \tau; V^B, \omega, \theta_l), d_{\bar{\sigma}}(V_t, \tau; V^B, \omega, \theta_h)\} < \varepsilon \text{ for all } V^B \leq \overline{V^B} \quad (C3)$$

for some large enough $\overline{V^B} < V_0$ and some arbitrarily small $\varepsilon > 0$. Then, for any $V^B \in (0, \overline{V^B})$, we can split the interval of integration of the inner integral on the RHS of equation C1 above into two disjoint intervals

$$[V^B, \infty) = [V^B, V^{max}) \cup [V^{max}, \infty)$$

and approximate $d_{\bar{\sigma}}(V, \tau - (s-t); V_{\bar{\sigma}}^B(\omega, \theta_h), \theta_l)$ by $b^{crf}(\tau - (s-t); r_{disc}, \omega)$ on $[V^{max}, \infty)$.

Armed with this, I let $v(V, V^B) \equiv \ln(V/V^B)$ and break the RHS of equation C1 into two terms:

$$J(V_t, \tau; V^B, \lambda, \omega, \theta) = J^{(1)}(V_t, \tau; V^{max}, V^B, \lambda, \omega, \theta) + J^{(2)}(V_t, \tau; V^{max}, V^B, \lambda, \omega, \theta)$$

where

$$\begin{aligned} J^{(1)}(V_t, \tau; V^{max}, V^B, \lambda, \omega, \theta) &\equiv \lambda \int_t^{t+\tau} e^{-(r_{disc}+\lambda)(s-t)} \left\{ \int_{V^B}^{V^{max}} d_{\bar{\sigma}}(V, \tau-s; V_{\bar{\sigma}}^B(\omega, \theta_h), \omega, \theta_l) \times \right. \\ &\quad \times \left[-\frac{\partial}{\partial V} \Psi^{v,t^d}(s-t, v(V; V^B); v(V_t; V^B), \sigma_l) \right] dV \Big\} \cdot ds \end{aligned} \quad (C4)$$

and

$$\begin{aligned} J^{(2)}(V_t, \tau; V^{max}, V^B, \lambda, \omega, \theta) &\equiv \lambda \int_t^{t+\tau} e^{-(r_{disc}+\lambda)(s-t)} \left\{ \int_{V^{max}}^{\infty} d_{\bar{\sigma}}(V, \tau-s; V_{\bar{\sigma}}^B(\omega, \theta_h), \omega, \theta_l) \times \right. \\ &\quad \times \left[-\frac{\partial}{\partial V} \Psi^{v,t^d}(s-t, v(V; V^B); v(V_t; V^B), \sigma_l) \right] dV \Big\} \cdot ds \end{aligned} \quad (C5)$$

Next, I approximate $J^{(2)}(\cdot; \cdot)$ by

$$\begin{aligned} \tilde{J}^{(2)}(V_t, \tau; V^{max}, V^B, \lambda, \omega, \theta) &\equiv \lambda \int_t^{t+\tau} e^{-(r_{disc}+\lambda)(s-t)} \left\{ \int_{V^{max}}^{\infty} b^{crf}(\tau - (t-s); r_{disc}, \omega) \times \right. \\ &\quad \times \left[-\frac{\partial}{\partial V} \Psi^{v,t^d}(s-t, v(V; V^B); v(V_t; V^B), \sigma_l) \right] dV \Big\} \cdot ds \end{aligned} \quad (C6)$$

C.2 Independence from the bond contract parameters

For computational purposes, I break down the formulas in equations C4 and C6 into sums of simpler terms. These terms are comprised of the following functions, which are independent of the bond contract \mathbf{b} parameters:

$$f_1^{(1)}(v_t, \tau; r_{disc}, \lambda, \sigma_l) \equiv \int_0^\tau \int_0^{v^{max}} \left\{ \lambda e^{-(r_{disc} + \lambda)u} \left[-\Psi_2^{v, t^d}(u, w; v_t, \sigma_l) \right] \right\} dw \cdot du \quad (C7)$$

$$f_2^{(1)}(v_t, \tau, b_l^h; r_{grow}, r_{disc}, \lambda, \sigma_l, \sigma_h) \equiv \int_0^\tau \int_0^{v^{max}} \left\{ \lambda e^{-(r_{disc} \cdot \tau + \lambda \cdot u)} \left(1 - F(\tau - u, w - b_l^h; (r_{grow}, \sigma_h)) \right) \right. \\ \left. \times \left[-\Psi_2^{v, t^d}(u, w; v_t, \sigma_l) \right] \right\} dw \cdot du \quad (C8)$$

$$f_3^{(1)}(v_t, \tau, b_l^h; r_{grow}, r_{disc}, \lambda, \sigma_l, \sigma_h) \equiv \int_0^\tau \int_0^{v^{max}} \left\{ \lambda e^{-(r_{disc} + \lambda)u} G(\tau - u, w - b_l^h; (r_{disc}, r_{grow}, \sigma_h)) \right. \\ \left. \times \left[-\Psi_2^{v, t^d}(u, w; v_t, \sigma_l) \right] \right\} dw \cdot du \quad (C9)$$

$$f_1^{(2)}(v_t, \tau; v^{max}, r_{disc}, \lambda, \sigma_l) \equiv \int_0^\tau \left\{ \lambda e^{-(r_{disc} + \lambda)u} \Psi^{v, t^d}(u, v^{max}; v_t, \sigma_l) \right\} du \quad (C10)$$

$$f_2^{(2)}(v_t, \tau; v^{max}, r_{disc}, \lambda, \sigma_l) \equiv \int_0^\tau \left\{ \lambda e^{-(r_{disc} \cdot \tau + \lambda \cdot u)} \Psi^{v, t^d}(u, v^{max}; v_t, \sigma_l) \right\} du \quad (C11)$$

where Ψ_2^{v, t^d} denotes the derivative of Ψ^{v, t^d} w.r.t. its second argument.

C.2.1 Decomposing $J^{(1)}$

I start by defining the following variables

$$w \equiv v(V, V_l^B) \quad (C12)$$

$$v_t \equiv v(V_t, V_l^B) \quad (C13)$$

$$v^{max} \equiv v(V^{max}, V_l^B) \quad (C14)$$

$$b_l^h \equiv v(V_{\bar{\sigma}}^B(\omega, \theta_h), V_l^B) \quad (C15)$$

where $v(a, b) \equiv \ln(a/b)$. This gives

$$V_{\bar{\sigma}}^B(\omega, \theta_h) = V_l^B e^{b_l^h}$$

and

$$\ln\left(\frac{V}{V_{\bar{\sigma}}^B(\omega, \theta_h)}\right) = \ln\left(\frac{V}{V_l^B}\right) + \ln\left(\frac{V_l^B}{V_{\bar{\sigma}}^B(\omega, \theta_h)}\right) = w - b_l^h$$

Substituting the formulas above and the post-volatility-shock bond price expression in equation C4, we obtain

$$J^{(1)}(v_t, \tau; V^{max}, V_l^B, \lambda, \omega, \theta) = \int_t^{t+\tau} \int_{V_l^B}^{V^{max}} \left\{ \frac{c}{r_{disc}} \times \lambda e^{(r_{disc} + \lambda)(s-t)} \left[-\frac{\partial}{\partial V} \Psi^{v, t^d}(s-t, w, v_t, \sigma_l) \right] \right. \\ \left. + \left[p - \frac{c}{r_{disc}} \right] \times \left(\lambda e^{-(r_{disc} \cdot \tau + \lambda \cdot (s-t))} (1 - F(\tau - (s-t), w - b_l^h; \theta_{0,h})) \right) \right\} dw \cdot ds$$

$$\begin{aligned}
& \times \left[-\frac{\partial}{\partial V} \Psi^{v,t^d}(s-t, w; v_t, \sigma_l) \right] \Bigg) \\
& + \left[\frac{\alpha V_{\bar{\sigma}}^B(\omega, \theta_h)}{m} - \frac{c}{r_{disc}} \right] \times \left(\lambda e^{-(r_{disc}+\lambda)(s-t)} G(\tau - (s-t), w - b_l^h; \theta_h) \right. \\
& \quad \left. \times \left[-\frac{\partial}{\partial V} \Psi^{v,t^d}(s-t, w; v_t, \sigma_l) \right] \right) \Bigg\} dV \cdot ds
\end{aligned} \tag{C16}$$

Now notice that

$$\frac{\partial}{\partial V} \Psi^{v,t^d}(s-t, w; v_t, \sigma_l) dV = \Psi_2^{v,t^d}(s-t, w; v_t, \sigma_l) \cdot \frac{1}{V}$$

and $dw = 1/V \cdot dV$. A simple change of variables then yields

$$\int_{V_l^B}^{V^{max}} \frac{\partial}{\partial V} \Psi^{v,t^d}(s-t, w; v_t, \sigma_l) dV = \int_0^{v^{max}} \Psi_2^{v,t^d}(s-t, w; v_t, \sigma_l) dw \tag{C17}$$

Applying this transformation to equation C16 above gives

$$\begin{aligned}
J^{(1)}(v_t, \tau; V^{max}, V_l^B, \lambda, \omega, \theta) &= \int_0^\tau \int_0^{v^{max}} \left\{ \frac{c}{r_{disc}} \times \lambda e^{-(r_{disc}+\lambda)u} \left[-\Psi_2^{v,t^d}(u, w; v_t, \sigma_l) \right] \right. \\
&\quad + \left[p - \frac{c}{r_{disc}} \right] \times \left(\lambda e^{-(r_{disc} \cdot \tau + \lambda \cdot u)} \left(1 - F(\tau - u, w - b_l^h; \theta_{0,h}) \right) \right. \\
&\quad \left. \left. \times \left[-\Psi_2^{v,t^d}(u, w; v_t, \sigma_l) \right] \right) \right. \\
&\quad + \left[\frac{\alpha V_{\bar{\sigma}}^B(\omega, \theta_h)}{m} - \frac{c}{r_{disc}} \right] \times \left(\lambda e^{-(r_{disc}+\lambda)u} G(\tau - u, w - b_l^h; \theta_h) \right. \\
&\quad \left. \left. \times \left[-\Psi_2^{v,t^d}(u, w; v_t, \sigma_l) \right] \right) \right\} dw \cdot ds
\end{aligned}$$

Substituting the f_i functions in the expression above finally gives

$$\begin{aligned}
J^{(1)}(v_t, \tau, b_l^h; v^{max}, \lambda, \omega, \theta) &= \frac{c}{r_{disc}} \times f_1^{(1)}(v_t, \tau; r_{disc}, \lambda, \sigma_l) \\
&\quad + \left[p - \frac{c}{r_{disc}} \right] \times f_2^{(1)}(v_t, \tau, b_l^h; r_{grow}, r_{disc}, \lambda, \sigma_l, \sigma_h) \\
&\quad + \left[\frac{\alpha V_{\bar{\sigma}}^B(\omega, \theta_h)}{m} - \frac{c}{r_{disc}} \right] \times f_3^{(1)}(v_t, \tau, b_l^h; r_{grow}, r_{disc}, \lambda, \sigma_l, \sigma_h)
\end{aligned} \tag{C18}$$

where I have adjusted the arguments of the $J^{(1)}$ function on the LHS accordingly.

C.2.2 Decomposing $\tilde{J}^{(2)}$

Notice that the credit-risk-free bond price b^{crf} can be taken out of the inner integral on the RHS of equation C6. The inner integral then becomes

$$-\int_{V^{max}}^\infty \frac{\partial}{\partial V} \Psi^{v,t^d}(s-t, v(V; V^B); v(V_t; V^B), \sigma_l) dV = -\Psi^{v,t^d}(s-t, v(V; V^B); v(V_t; V^B), \sigma_l) \Big|_{V=V^{max}}^\infty$$

$$\begin{aligned}
& - \lim_{V \rightarrow \infty} \Psi^{v,t^d}(s-t, v(V; V^B); v(V_t; V^B), \sigma_l) + \\
& + \Psi^{v,t^d}(s-t, v(V^{max}; V^B); v(V_t; V^B), \sigma_l) \\
& = \Psi^{v,t^d}(s-t, v(V^{max}; V^B); v(V_t; V^B), \sigma_l)
\end{aligned}$$

Plugging this expression into the formula for $\tilde{J}^{(2)}$ yields

$$\begin{aligned}
\tilde{J}^{(2)}(V, \tau; V^{max}, V^B, \lambda, \omega, \theta) &= \lambda \int_t^{t+\tau} \left\{ e^{-(r_{disc}+\lambda)(s-t)} \cdot b^{crf}(\tau - (t-s)) \times \right. \\
& \quad \left. \times \Psi^{v,t^d}(s-t, v(V^{max}; V^B); v(V_t; V^B), \sigma_l) \right\} ds \quad (C19)
\end{aligned}$$

Setting t to 0 and substituting the credit-risk-free bond price b^{crf} for the formula in equation C2 then gives

$$\begin{aligned}
\tilde{J}^{(2)}(V, \tau; V^{max}, V^B, \lambda, \omega, \theta) &= \lambda \int_0^\tau \left\{ e^{-(r_{disc}+\lambda)u} \left[\frac{c}{r_{disc}} + e^{-r_{disc}(\tau-u)} \left(p - \frac{c}{r_{disc}} \right) \right] \times \right. \\
& \quad \left. \times \Psi^{v,t^d}(u, v(V^{max}; V^B); v(V_t; V^B), \sigma_l) \right\} du \\
&= \frac{c}{r_{disc}} \int_0^\tau \lambda e^{-(r_{disc}+\lambda)u} \Psi^{v,t^d}(u, v(V^{max}; V^B); v(V_t; V^B), \sigma_l) ds \\
& \quad + \left(p - \frac{c}{r_{disc}} \right) \int_0^\tau \lambda e^{-(r_{disc} \cdot \tau + \lambda \cdot u)} \Psi^{v,t^d}(u, v(V^{max}; V^B); v(V_t; V^B), \sigma_l) du \quad (C20)
\end{aligned}$$

Finally, by equations C10 to C15, we get

$$\tilde{J}^{(2)}(v_t, \tau; v^{max}, \lambda, \omega, \theta_l) = \frac{c}{r_{disc}} \times f_1^{(2)}(v_t, \tau; v^{max}, r_{disc}, \lambda, \sigma_l) + \left[p - \frac{c}{r_{disc}} \right] \times f_2^{(2)}(v_t, \tau; v^{max}, r_{disc}, \lambda, \sigma_l) \quad (C21)$$

C.2.3 The Approximated Double Integral Formula

By equations C18 and C21, the double integral term in pre-volatility-shock bond pricing formula can be approximated by:

$$\begin{aligned}
J(V_t, \tau; V_t^B, \lambda, \omega, \theta) &\approx J^{(1)}(v_t, \tau, b_l^h; v^{max}, \lambda, \omega, \theta) + \tilde{J}^{(2)}(v_t, \tau; v^{max}, \lambda, \omega, \theta_l) \\
&= \frac{c}{r_{disc}} \times f_1^{(1)}(v_t, \tau; r_{disc}, \lambda, \sigma_l) \\
& \quad + \left[p - \frac{c}{r_{disc}} \right] \times f_2^{(1)}(v_t, \tau, b_l^h; r_{grow}, r_{disc}, \lambda, \sigma_l, \sigma_h) \\
& \quad + \left[\frac{\alpha V_{\bar{\sigma}}^B(\omega, \theta_h)}{m} - \frac{c}{r_{disc}} \right] \times f_3^{(1)}(v_t, \tau, b_l^h; r_{grow}, r_{disc}, \lambda, \sigma_l, \sigma_h) \\
& \quad + \frac{c}{r_{disc}} \times f_1^{(2)}(v_t, \tau; v^{max}, r_{disc}, \lambda, \sigma_l) \\
& \quad + \left[p - \frac{c}{r_{disc}} \right] \times f_2^{(2)}(v_t, \tau; v^{max}, r_{disc}, \lambda, \sigma_l) \quad (C22)
\end{aligned}$$

C.3 Numerical Computation of the \mathbf{b} -independent f functions

This section discusses the computation of the $f_j^{(i)}$ functions defined in equations C7 to C11. As pointed out in the previous section, these functions do not depend on the bond contract \mathbf{b} parameters. Once computed, they can be used to calculate the pre-volatility bond price for a wide range of coupon c , principal p and pre-shock default barrier V_l^B . The numerical approach does depend on the bond maturity, though, as explained below.

I start by forming a grid for v_t , τ and the ratio of the post- and pre-volatility-shock default barriers v_l^h :

$$v_l^h \equiv e^{b_l^h} = \frac{V_h^B}{V_l^B}$$

Since the underlying value of assets V never falls below an endogenously determined bankruptcy barrier $V^B > 0$, the lower bound for v_t is 0. The upper bound for this variable, v^{max} , should be set to a large enough value so that the approximation to the $J^{(2)}$ term discussed above holds. One way of doing so is to find V^{max} satisfying condition C3 when the default barrier V^B is set to the initial asset value V_0 . Then

$$G_v \equiv \{v_1, v_2, \dots, v_{N_v}\}$$

where $v_0 = 0$ and $v_{N_v} = v^{max}$. I set the maximum time-to-maturity τ to the bond maturity m , so that

$$G_\tau \equiv \{\tau_1, \tau_2, \dots, \tau_{N_\tau}\}$$

where $\tau_0 = 0$ and $\tau_{N_\tau} = m$. Finally, I arbitrarily set the minimum and maximum v_l^h values to $\underline{v_l^h}$ and $\overline{v_l^h}$. The bankruptcy barriers vary with the bond contract parameters, but their ratio depends mostly on the shock size, $\sigma_h - \sigma_l$. Numerical tests suggest that this ratio is generally contained in the interval $[0.5, 1.5]$. Therefore, I set

$$G_l^h \equiv \{v_{l,1}^h, v_{l,2}^h, \dots, v_{l,N_l^h}^h\}$$

where $v_{l,0}^h = \underline{v_l^h}$ and $v_{l,N_l^h}^h = \overline{v_l^h}$.

Finally, given the grids above, I compute the integrands of the double integrals in the $f_j^{(i)}$ formulas for each combination of w , τ and $\exp(v_l^h)$. The exception is the case of $f_1^{(1)}$, with which I deal separately, as discussed below. I am left with the multidimensional arrays listed in Table I.

Table I: Table to test captions and labels

Integrand Matrix	Function	Arguments	Fixed Parameters	Dimensions
$F_2^{(1)}$	$f_2^{(1)}$	$v_t, \tau, e^{v_l^h}$	$r_{grow}, r_{disc}, \lambda, \sigma_l, \sigma_h$	$N_v \times N_\tau \times N_l^h$
$F_3^{(1)}$	$f_3^{(1)}$	$v_t, \tau, e^{v_l^h}$	$r_{grow}, r_{disc}, \lambda, \sigma_l, \sigma_h$	$N_v \times N_\tau \times N_l^h$
$F_1^{(2)}$	$f_1^{(2)}$	v_t, τ	$r_{disc}, \lambda, \sigma_l, \sigma_h$	$N_v \times N_\tau$
$F_2^{(2)}$	$f_2^{(2)}$	v_t, τ	$r_{disc}, \lambda, \sigma_l$	$N_v \times N_\tau$

C.3.1 Computing function $f_1^{(1)}$

Because τ appears only as the upper limit of integration of the outer integral on the RHS of equation C7, there is no need to recalculate the integrand every time τ changes. Instead, I compute

first the inner integral

$$g_1^{(1)}(v_t, u; v^{max}, r_{disc}, \lambda, \sigma_l) \equiv \int_0^{v^{max}} \left\{ \lambda e^{-(r_{disc} + \lambda)u} \left[-\Psi_2^{v, t^d}(u, w; v_t, \sigma) \right] \right\} dw \quad (C23)$$

for each pair (v_t, u) in $G_v \times G_\tau$. Given a pair (v_t, u) , I compute the integrand for each w value in G_v and fit a one-dimensional cubic spline to the resulting array. I then approximate the integral by the following summation

$$g_1^{(1)}(v_t, u; v^{max}, r_{disc}, \lambda, \sigma_l) \approx \sum_{j=1}^{N_w} \left\{ \lambda e^{-(r_{disc} + \lambda)u} \left[-\Psi_2^{v, t^d}(u, w_j; v_t, \sigma) \right] \right\} dw$$

using a refined, equally-spaced grid of v -values, $\{w_j\}_{j=0}^{N_w}$, with $w_0 = 0$, $w_{N_w} = v^{max}$, $N_w \gg N_v$ and $dw = w_{j+1} - w_j$, $j \geq 1$.

For each v_t in G_v , I am left with the array

$$\begin{bmatrix} g_1(v_t, \tau_1; v^{max}, r_{disc}, \lambda, \sigma_l) \\ g_1(v_t, \tau_2; v^{max}, r_{disc}, \lambda, \sigma_l) \\ \vdots \\ g_1(v_t, \tau_N; v^{max}, r_{disc}, \lambda, \sigma_l) \end{bmatrix}$$

to which I fit a one-dimensional cubic spline to obtain a function of τ , $f_1^{(1)}(\tau; v_t, v^{max}, r_{disc}, \lambda, \sigma_l)$. This function can then be used to back-out

$$f_1(v_t, \tau; v^{max}, r_{disc}, \lambda, \sigma_l) = \int_0^\tau \int_0^{v^{max}} \left\{ \lambda e^{-(r_{disc} + \lambda)u} \left[-\Psi_2^{v, t^d}(u, w; v_t, \sigma) \right] \right\} dw \cdot du$$

for any $\tau \in [0, m]$.

C.4 Calculating the Vector of Bond Prices in the Finite Difference Methods for the Equity Function

Form a grid of v_t values in $[0, v^{max}]$. Next, compute the interpolated \tilde{f}_i , $i = 1, 2, 3, 4$, above at each (v_t, τ, b_l^h) tuple and use them to calculate bond prices.

DOUBLE-CHECK!

$$\begin{aligned} d_\lambda(v_t, \tau, b_l^h; v^{max}, \lambda, \omega, \theta) &\approx \frac{c}{r_{disc} + \lambda} + e^{-(r_{disc} + \lambda)\tau} \left[p - \frac{c}{r_{disc} + \lambda} \right] [1 - F(\tau, v_t; \sigma_l)] ls \\ &+ \left[\frac{\alpha V_{\bar{\sigma}}^B(\omega, \theta_h) e^{-b_l^h}}{m} - \frac{c}{r_{disc} + \lambda} \right] G(\tau, v_t; \theta_l) \\ &+ J^{(1)}(v_t, \tau, b_l^h; v^{max}, \lambda, \theta) + \tilde{J}^{(2)}(v_t, \tau; v^{max}, \lambda, \theta_l) \end{aligned}$$

Now we can interpolate $d_\lambda(v_t, m, b_l^h; \lambda, \theta)$ in v_t and b_l^h .

Appendix D. Numerical Approach to Joint Equilibria

D.1 Full Information Module

Figure 11. Full Information-Module

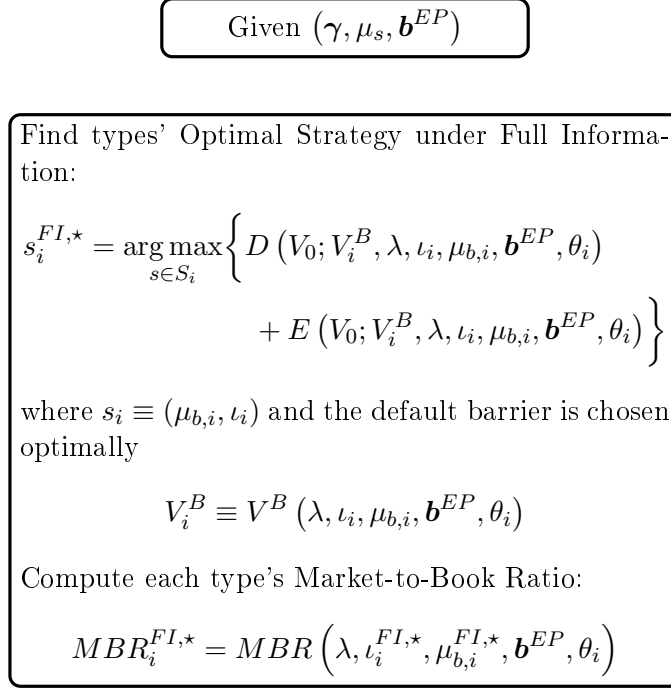
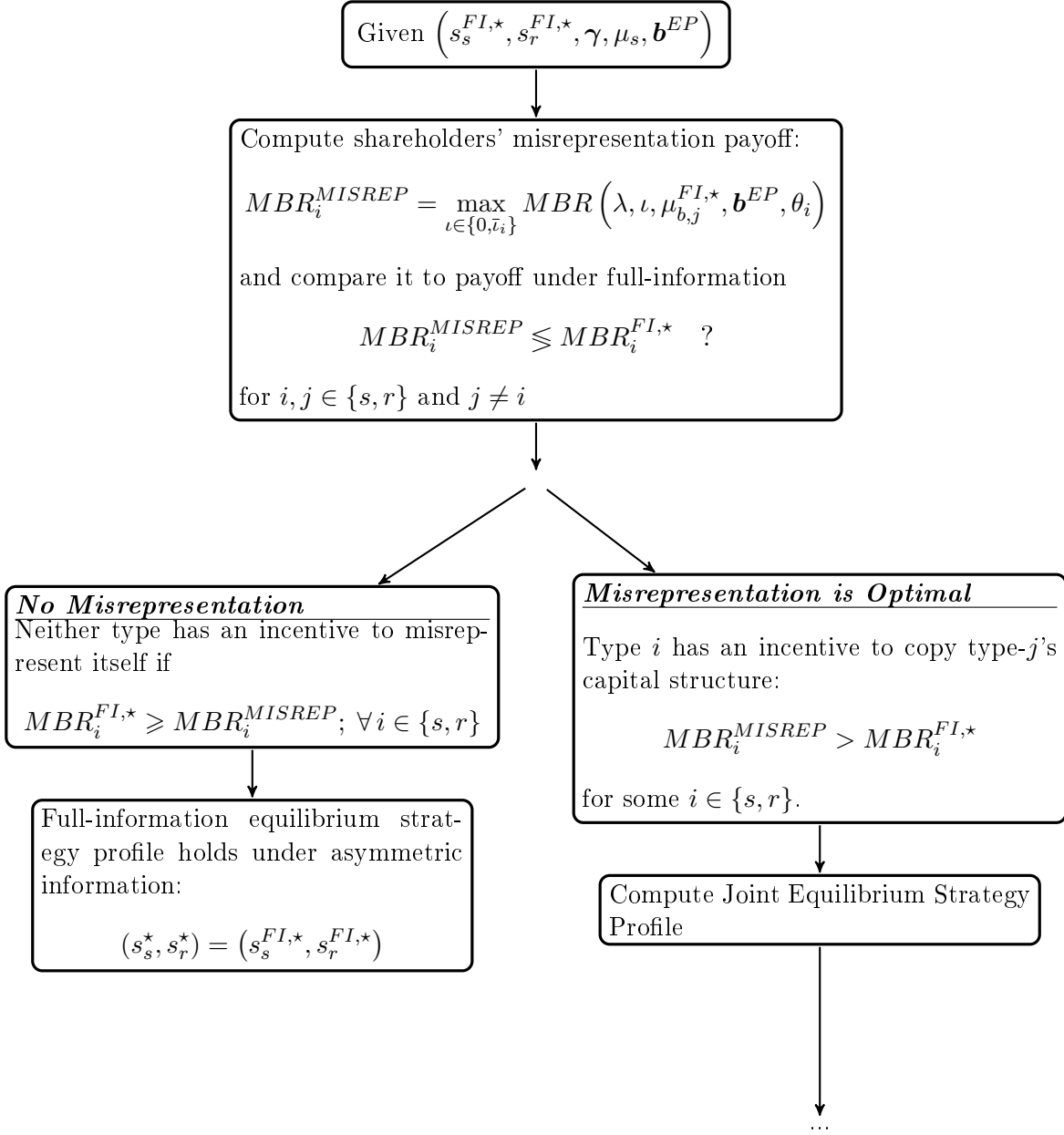
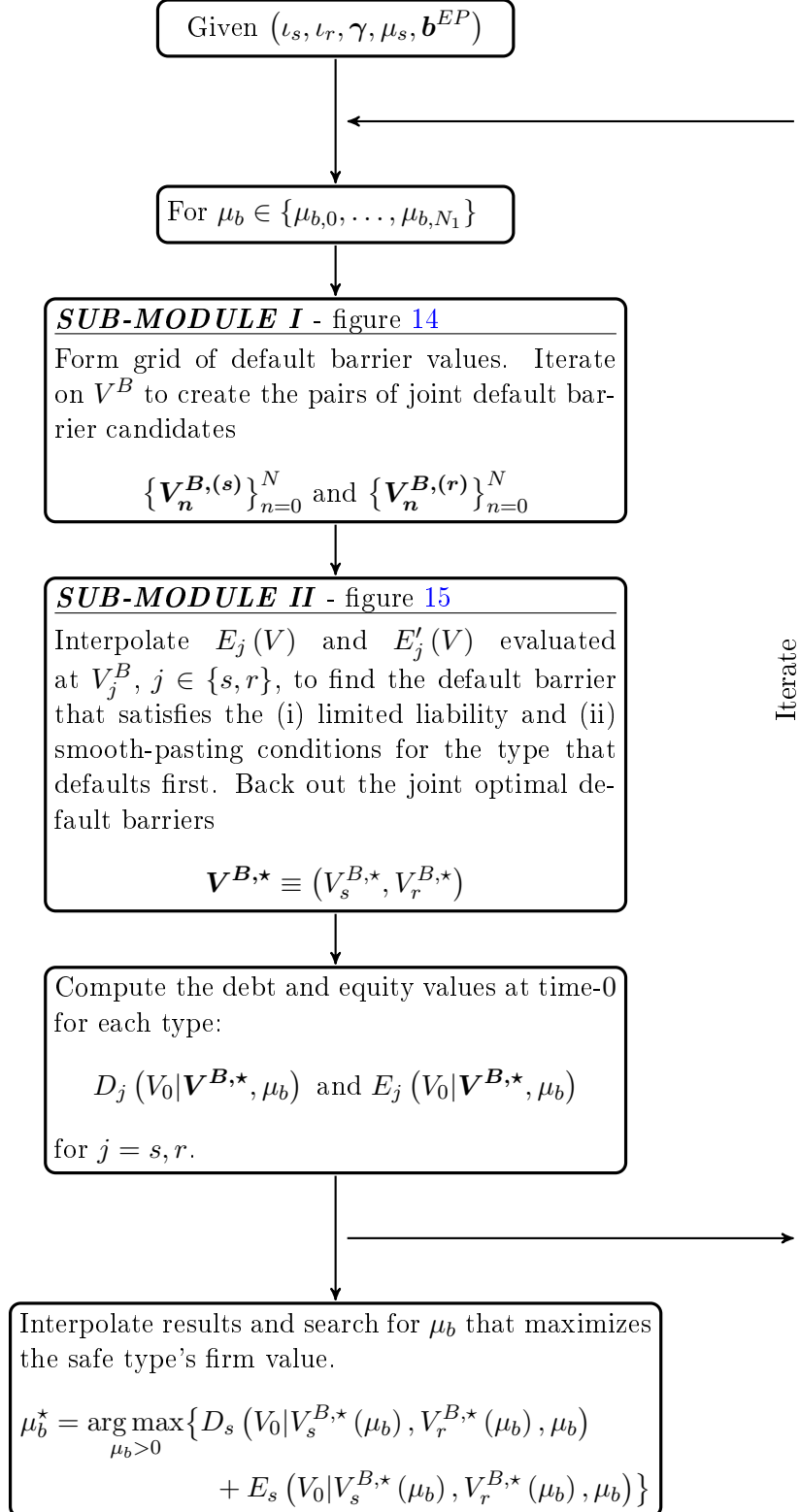


Figure 12. Misrepresentation-Module

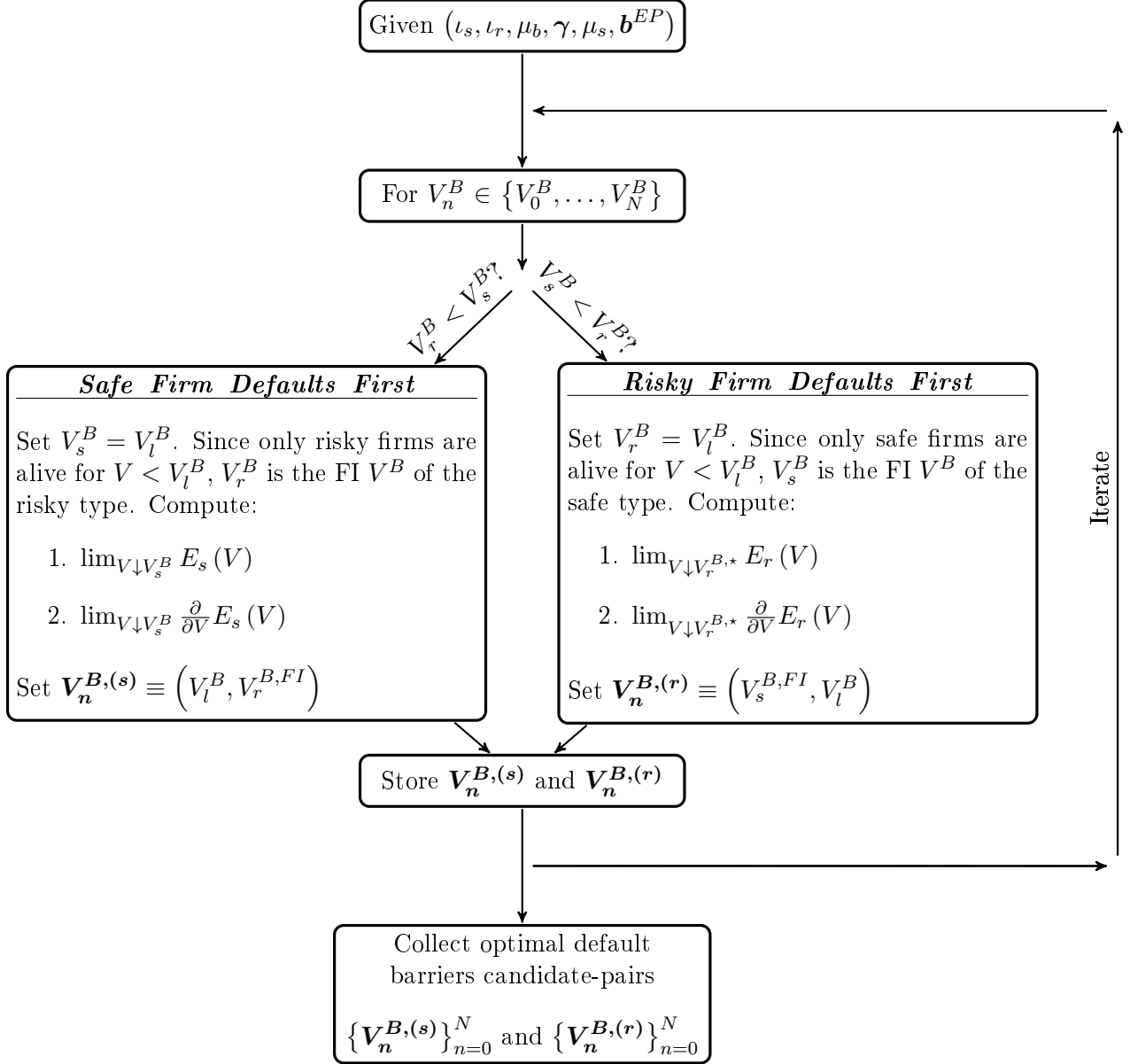


D.3 μ_b -Module

Figure 13. μ_b -Module: Numerical Computation of the Optimal Leverage



Given (i) the distribution of firms, (γ, μ_s) , (ii) the bond contract, \mathbf{b}^{EP} , and (iii) a pair of RMP choices, (ι_s, ι_r) , the optimal joint measure of outstanding bonds is computed as follows. For each value μ_b in a grid, derive the safe- and risky-type's optimal default barriers (sub-modules I and II). Next, imposing the optimal bankruptcy condition, price each type's debt and equity values at time-0. Having done so for all values in the grid, interpolate the time-0 debt and equity values and search for the joint measure of outstanding bonds that maximizes the safe-type's firm value.

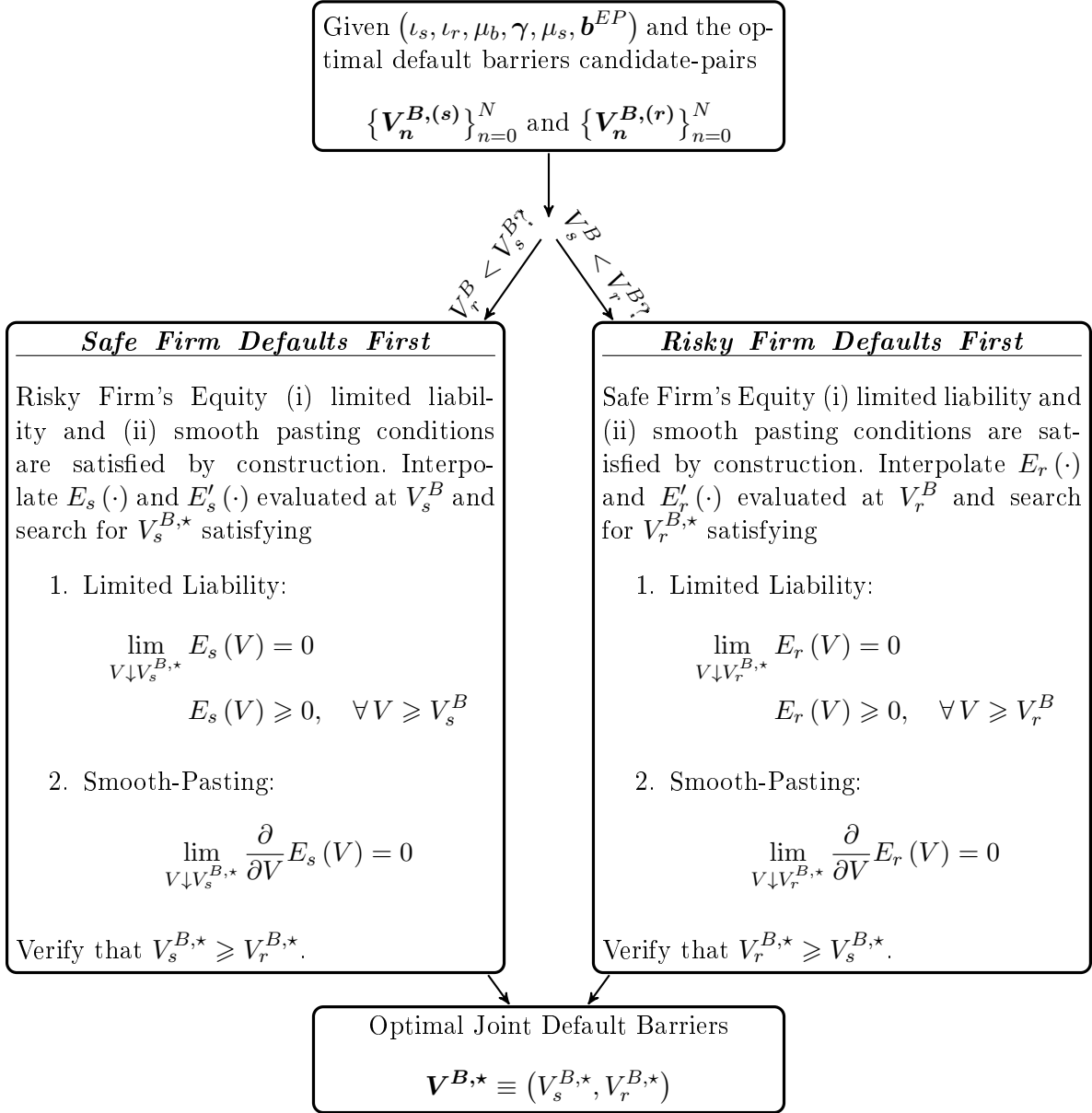
Figure 14. Sub-Module I - Iteration on V^B -candidates


Given (i) the distribution of firms, (γ, μ_s) , (ii) the bond contract, \mathbf{b}^{EP} , (iii) a pair of RMP choices, (ι_s, ι_r) , and (iv) an arbitrary joint measure of outstanding bonds, μ_b , the optimal default barriers candidate-pairs, \mathbf{V}_n^B , are computed as follows. For each bankruptcy threshold V^B in a grid, consider both the scenario in which risky-type firms default before safe-type firms do and the opposite case. If type- i defaults before type- j , $V_i^B > V_j^B$. Since, by assumption, only type- j firms are still alive at $V = V_i^B$, the information asymmetry disappears the moment the value of assets of a type- j firm crosses the type- i 's bankruptcy barrier from above for the first time. Thereafter, the bonds issued by such type- j firm are priced according to the full-information formulas in Theorems ??correct reference and ?. From this it follows that the default barrier of the last-

to-default-type in a joint equilibrium coincides with its bankruptcy choice under full-information (FI). Having set the last-to-default-type's default barrier to $V_j^{B,FI}$, compute type- i 's equity value and equity derivative evaluated at the proposed default barrier, V_n^B . For each value in the grid, the algorithm returns two pairs of bankruptcy thresholds, one for each bankruptcy case, $V_s^B \geq V_r^B$ and $V_s^B < V_r^B$.

D.5 Sub-Module II

Figure 15. Sub-Module II - Interpolation to Back out Optimal Default Barriers.



Given (i) the distribution of firms, (γ, μ_s) , (ii) the bond contract, \mathbf{b}^{EP} , (iii) a pair of RMP choices, (ι_s, ι_r) , (iv) an arbitrary joint measure of outstanding bonds, μ_b , and (v) the optimal default barriers candidate-pairs, $\{\mathbf{V}_n^{B,(s)}\}_{n=0}^N$ and $\{\mathbf{V}_n^{B,(r)}\}_{n=0}^N$ obtained in sub-module I (figure 14), the optimal default barriers are computed as follows. For the case where type- i defaults before type- j , type- j 's default barrier is fixed at $V_j^{B,FI}$. Compute type- i 's equity and equity derivative evaluated at $V = V_{i,n}^B$ for each pair in $\{\mathbf{V}_n^{B,(i)}\}_{n=0}^N$. Interpolate these functions and search for $V_i^{B,*}$ such that type- i 's equity limited liability and smooth pasting conditions are satisfied. (technical note: since the value of equity at the default barrier is set to zero by construction in the finite-differences method, to impose the limited liability condition, search for the value of $V_i^{B,*}$ such that the minimum

type- i equity value other than zero is non-negative and sufficiently close to zero when the default barriers are V_i^B and $V_j^{B,FI}$.) If $V_i^B > V_j^{B,FI}$ and type- j 's equity value is positive for $V \geq V_j^{B,FI}$, the pair satisfies the optimality conditions. Typically, only the case where the risky type defaults first will yield a result.